Inorg. Chem. **2003**, *42*, 5579–5593

Nickel(II) Complexes of 21-C-Alkylated Inverted Porphyrins: Synthesis, Protonation, and Redox Properties

Izabela Schmidt and Piotr J. Chmielewski*

Department of Chemistry, University of Wrocław, F. Joliot-Curie Street 14, 50 383 Wrocław, Poland

Received January 29, 2003

Reaction of the nickel(II) complex of an inverted porphyrin, (5,10,15,20-tetraphenyl-2-aza-21-carbaporphyrinato)-nickel(II) (**1**), with haloalkanes in the presence of proton scavengers yields 21-C-alkylated complexes. The products are separated and characterized spectroscopically. Chirality of the formed substituted metalloporphyrins is discussed on the basis of the ^{1}H NMR spectra. Diastereomers are observed for the complexes containing chiral substituents. Protonation of the external nitrogen of the inverted pyrrole is combined with coordination of the apical ligand that leads to paramagnetic nickel(II) complexes. Very strong differentiation of the isotropic shift for diastereotopic methylene protons is observed in ^{1}H NMR spectra of the protonated paramagnetic species. For the systems containing benzyl, allyl, and ethoxymethyl substituents a mild dealkylation in solution of protonated complexes is observed in the presence of oxygen. Redox properties of the alkylated complexes are studied by means of cyclic voltammetry. Oxidation of the nickel center in 21-alkylated systems takes place at the potentials comparable to that of unsubstituted complex **1**. Protonation introduces small changes to the potential of the Ni^{II}/Ni^{III} redox couple, but it stabilizes nickel(I) species. Products of chemical oxidation and reduction of the alkylated complexes are detected by means of the EPR spectroscopy indicating in both cases metal-centered redox processes.

Introduction

The group of porphyrin analogues consists of a variety of aromatic macrocyclic compounds containing pyrrole subunits. Programmed synthesis of a particular macrocycle allows profound alteration or fine-tuning of the optical, acid−base, or coordinating properties with regard to its potential usability in medicine, photochemistry, molecular electronics, catalysis, etc.[1] Among the analogues are the core-modified porphyrins in which at least one of the nitrogen atoms is substituted by another element. In this class there are mono- and diheteroporphyrins[2] containing oxygen, sulfur, selenium, and tellurium atom(s) in the macrocyclic interior. Such a substitution changes an overall charge of the macrocyclic ligand and consequently alters properties of the metal complexes since a heteroatom replaces the NH group of the porphyrin.

A special set of aromatic, porphyrin-related compounds is constituted by macrocycles identified by the presence of a CH motif in the macrocyclic interior. Among them are carbaporphyrins with one[3] or two[4] pyrrole rings replaced by an all-carbon ring(s), so-called inverted or *N*-confused porphyrins that are isomers of porphyrins,[5] doubly *N*-confused porphyrin,[6] and isomers of oxa-, thia-, dithia-, and selenaporphyrins.[7]

The attractiveness of these macrocycles comes from their potential ability to form carbon−metal bonds. Such organometallic coordination may be additionally stabilized by

* To whom correspondence should be addressed. E-mail: pjc@wchuwr.chem.uni.wroc.pl.

(1) (a) Jasat, A.; Dolphin, D. *Chem. Rev.* **1997**, *97*, 2267. (b) Sessler, J. L.; Gebauer, A.; Vogel, E. In *The Porphyrin Handbook*; Kadish, K. M., Smith, K. M., Guilard, R., Eds.; Academic Press: New York, 2000; Vol. 2, Chapter 8.

(2) (a) Latos-Grażyński, L. In *The Porphyrin Handbook*; Kadish, K. M., Smith, K. M., Guilard, R., Eds.; Academic Press: New York, 2000; Vol. 2, p 361. (b) Pacholska, E.; Latos-Grażyński, L.; Ciunik, Z. *Angew. Chem., Int. Ed.* **2001**, *40*, 4466.

(3) (a) Berlin, K.; Breitmaier, E. *Angew. Chem., Int. Ed. Engl.* **1994**, *33*, 1246. (b) Lash, T. D. *Angew. Chem., Int. Ed. Engl.* **1995**, *34*, 2533. (c) Lash, T. D.; Chaney, S. T. *Tetrahedron Lett.* **1996**, *37*, 8825. (d) Lash, T. D.; Chaney, S. T. *Angew. Chem., Int. Ed. Engl.* **1997**, *36*, 840. (e) Berlin, K. *Angew. Chem., Int. Ed. Engl.* **1996**, *35*, 1820. (f) Hayes, M. J.; Lash, T. D. *Chem.—Eur. J.* **1998**, *4*, 508. (g) Lash, T. D.; Chaney, S. T. *Chem.—Eur. J.* **1996**, *2*, 944. (h) Lash, T. D.; Hayes, M. J. *Angew. Chem., Int. Ed. Engl.* **1997**, *36*, 840. (i) Lash, T. D. *Chem. Commun.* **1998**, 1683. (j) Lash, T. D.; Chaney, S. T.; Richter, D. T. *J. Org. Chem.* **1998**, *63*, 9076. (k) Hayes, M. J.; Spence, J. D.; Lash, T. D. *Chem. Commun.* **1998**, 2409. (l) Lash, T. D. *Synlett* **2000**, 279. (m) Richter, D. T.; Lash, T. D. *Tetrahedron* **2001**, *57*, 3659. (n) Lash, T. D.; Hayes, M. J.; Spence, J. D.; Muckey, M. A.; Ferrence, G. M.; Szczepura, L. F. *J. Org. Chem.* **2002**, *67*, 4860. (o) Graham, S. R.; Colby, D. A.; Lash, T. D. *Angew. Chem., Int. Ed.* **2002**, *41*, 1371. (p) Colby, D. A.; Lash, T. D. *Chem.—Eur. J.* **2002**, *8*, 5397. (q) Liu, D.; Lash, T. D. *Chem. Commun.* **2002**, 2426.

10.1021/ic034096k CCC: $25.00
Published on Web 08/05/2003

the macrocyclic effect as well as by aromatic system of the porphyrinoid allowing observation of systems that are otherwise unstable. The interest in coordination chemistry of carbaporphyrinoids is growing rapidly. To date inverted porphyrin[5a,d,8] and doubly *N*-confused[6,9] porphyrin as well as benzi-,[10] oxybenzi-,[11] benzocarba-, and azuliporphyrin[12] have been shown to form stable complexes with transition metal ions. In the complexes of the inverted porphyrin the *N*-confused pyrrole can play a different roles depending on the metal ion, its oxidation state, or the method of the complex synthesis.[8] The external nitrogen can be free[8c,d] or proton-bearing.[5a,e,8a,b,e,f,h] It can also be involved in coordination.[8e,g,i,j] The internal carbon can be bonded to a metal ion in several different ways.[5a,e,8b,f,h] Depending on the number of protons leaving the macrocycle upon coordination, the ligand can act as a mono-, di-, or trianion which can compensate for charge on the metal ion. Such a variety of coordination modes makes the inverted porphyrin versatile and unique.

Discovery of the *meso*-tetraaryl-substituted inverted porphyrins among the products of the Rothemund synthesis mixture[5a,b] and subsequent optimization of the synthesis[5e] with respect to the inverted porphyrin make this macrocycle a readily obtainable and therefore attractive subject of studies and modifications (Chart 1). The inverted pyrrole is particularly reactive having an exposed nitrogen atom that can be protonated,[5a] methylated,[13] or fused in the porphyrin interior.[14] The tautomeric form of the macrocycle containing protonated external nitrogen[15] is susceptible to reaction in position 3, i.e., on the external carbon atom in the vicinity of the outer nitrogen.[16] A facile autoxidation of the ethyl substituent attached to this position leads to 3-hydroxyethyl and 3-acetyl derivatives of inverted porphyrin.[17] Both proton-bearing carbons of inverted pyrrole can be brominated,[14] and nitration of its internal carbon takes place under mild conditions.[18]

Chart 1. Inverted Porphyrin and Its Derivatives

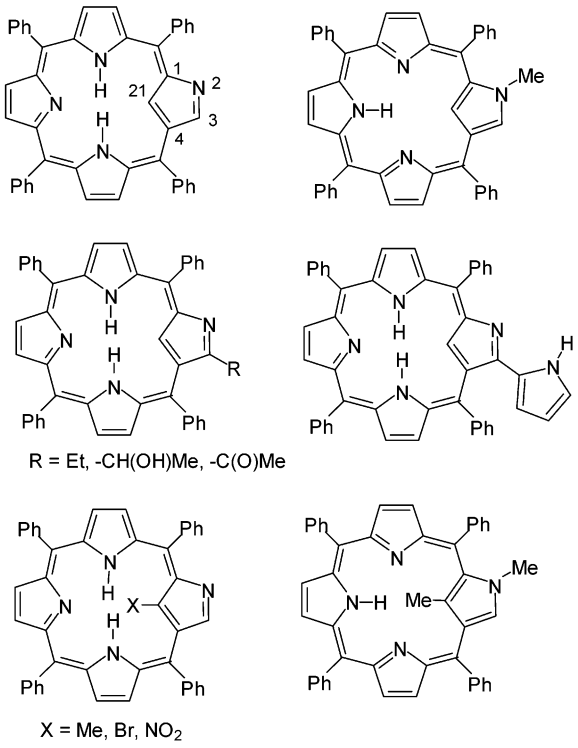

A particularly promising and simple method of modification of inverted porphyrins is related to the reactivity of the inverted pyrrole in metal complexes where the coordinating carbon is deprotonated. It has been shown that methylation of the internal carbon is possible for nickel(II)[19] and copper(II)[8b] complexes under mild conditions. Also, the dienophilic activity of the inverted pyrrole in the nickel(II) complex of inverted porphyrin has been reported recently.[20]

Alkylated inverted porphyrins are isomeric with their regular analogues. The *N*-alkylated porphyrins and their metal complexes have long been known and studied in the context of their significance in heme metabolism. Many different synthetic approaches were applied to modify the porphyrinic interior with various *N*-alkyl substituents.[21]

In this paper we report the results of our study on the alkylation of the nickel(II) complex of inverted porphyrin

(4) Lash, T. D.; Romanic, J. L.; Hayes, M. J.; Spence, J. D. *Chem. Commun.* **1999**, 819.

(5) (a) Chmielewski, P. J.; Latos-Grażyński, L.; Rachlewicz, K.; Glowiak, T. *Angew. Chem., Int. Ed. Engl.* **1994**, *33*, 779. (b) Furuta, H.; Asano, T.; Ogawa, T. *J. Am. Chem. Soc.* **1994**, *116*, 767. (c) Liu, B. Y.; Brückner, C.; Dolphin, D. *Chem. Commun*. **1996**, 2141. (d) Lash, T. D.; Richter, D. T.; Shiner, C. M. *J. Org. Chem.* **1999**, *64*, 7973. (e) Geier, G. R., III; Haynes, D. M.; Lindsey, J. S. *Org. Lett.* **1999**, *1*, 1455.

(6) Furuta, H.; Maeda, H.; Osuka, A. *J. Am. Chem. Soc*. **2000**, *122*, 803.

(7) (a) Heo, P. Y.; Shin, K.; Lee, C.-H. *Tetrahedron Lett.* **1995**, *37*, 197. (b) Lee, C.-H.; Kim, H.-J. *Tetrahedron Lett.* **1997**, *38*, 3935. (c) Lee, C.-H.; H. J.; Yoon, D.-W. *Bull. Korean Chem. Soc.* **1999**, *20*, 276. (d) Sprutta, N.; Latos-Grażyński, L. *Tetrahedron Lett*. **1999**, *40*, 8457. (e) Pacholska, E.; Latos-Grażyński, L.; Szterenberg, L.; Ciunik, Z. *J. Org. Chem*. **2000**, *65*, 8188. (f) Sprutta, N.; Latos-Grażyński, L. *Org. Lett.* **2001**, *3*, 1933.

(8) (a) Chmielewski, P. J.; Latos-Grażyński, L. *Inorg. Chem.* **1997**, *36*, 840. (b) Chmielewski, P. J.; Latos-Grażyński, L.; Schmidt, I. *Inorg. Chem.* **2000**, *39*, 5475. (c) Furuta, H.; Ogawa, T.; Uwatoko, Y.; Araki, K. *Inorg. Chem.* **1999**, *38*, 2676. (d) Ogawa, T.; Furuta, H.; Takahashi, M.; Morino, A.; Uno, H. *J. Organomet. Chem*. **2000**, *661*, 551. (e) Furuta, H.; Kubo, N.; Maeda, H.; Ishizuka, T.; Osuka, A.; Nanami, H.; Ogawa, T. *Inorg. Chem*. **2000**, *39*, 5424. (f) Chen, W.-C.; Hung, C.-H. *Inorg. Chem.* **2001**, *40*, 5070. (g) Srinivasan, A.; Furuta, H.; Osuka, A. *Chem. Commun.* **2001**, 1666. (h) Bohle, D. S.; Chen W. C.; Hung, C. H. *Inorg. Chem.* **2002**, *41*, 3334. (i) Harvey, J. D.; Ziegler, C. J. *Chem. Commun.* **2002**, 1942. (j) Hung, C.-H.; Chen, W.-C.; Lee, G.-H.; Peng, S.-M. *Chem. Commun.* **2002**, 1516.

(9) (a) Furuta, H.; Maeda, H.; Osuka, A. *Chem. Commun*. **2000**, *1143*. (b) Araki, K.; Winnischofer, H.; Toma, H. E.; Maeda, H.; Osuka, A.; Furuta, H. *Inorg, Chem.* **2001**, *40*, 2020.

(10) Stępień, M.; Latos-Grażyński, L. *Chem.—Eur. J.* **2001**, *7*, 5113.

(11) Stępień, M.; Latos-Grażyński, L.; Lash, T. D.; Szterenberg, L. *Inorg. Chem.* **2001**, *40*, 6892.

(12) (a) Graham, S. R.; Ferrence, G. M.; Lash, T. D. *Chem. Commun*. **2002**, 894. (b) Muckey, M. A.; Szczepura, L. F.; Ferrence, G. M.; Lash, T. D. *Inorg. Chem*. **2002**, *41*, 4840.

(13) Chmielewski, P.; Latos-Grażyński, L. *J. Chem. Soc., Perkin Trans. 2* **1995**, 503.

(14) Furuta, H.; Ishizuka, T.; Osuka, A.; Ogawa, T. *J. Am. Chem. Soc.* **2000**, *122*, 5748.

(15) (a) Furuta, H.; Ishizuka, T.; Osuka, A.; Dejima, H.; Nakagawa, H.; Ishikawa, Y. *J. Am. Chem. Soc*. **2001**, *123*, 6207.

(16) Schmidt, I.; Chmielewski, P. J. *Tetrahedron Lett*. **2001**, *42*, 1151.

(17) Schmidt, I.; Chmielewski, P. J. *Tetrahedron Lett*. **2001**, *42*, 6389.

(18) Ishikawa, Y.; Yoshida, I., Akaiwa, K.; Koguchi, E.; Sasaki, T.; Furuta, H. *Chem. Lett.* **1997**, 453.

(19) Chmielewski, P. J.; Latos-Grażyński, L.; Głowiak, T. *J. Am. Chem. Soc*. **1996**, *118*, 5690.

(20) Xiao, Z.; Patrick, B. O.; Dolphin, D. *Chem. Commun.* **2002**, 1816.

(21) Lavalee, D. K. *The Chemistry and Biochemistry of N-Substituted Porphyrins*: VCH Publishers: Weinheim, Germany, 1987.

Scheme 1. Alkylation of Nickel(II) Complex of Inverted Porphyrin with Monohaloalkanes

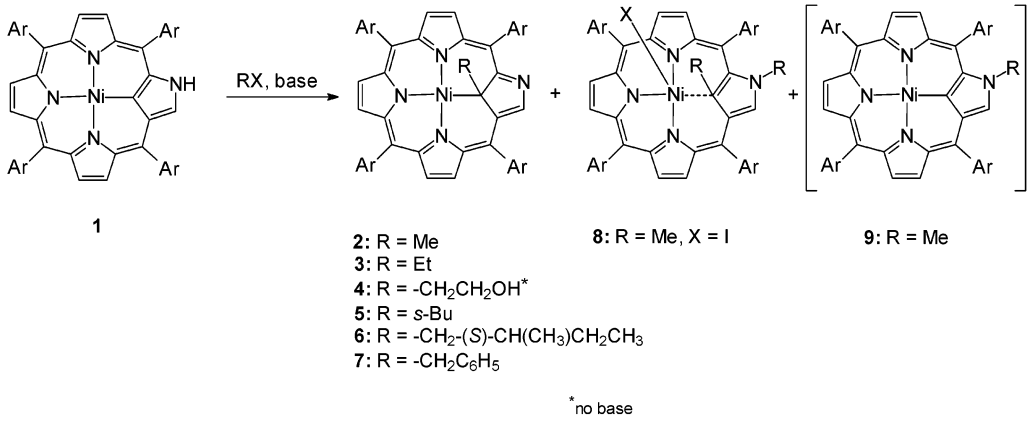

using a selection of alkylating agents. We concentrate here on the selectivity of the reaction with respect to the 21-monoalkylated product, chirality of the alkylated complexes, and ability of the nickel center to change its spin and oxidation states.

Results and Discussion

Syntheses. The general procedure involves addition of an excess of RX to the solution of **1** in dichloromethane, chloroform, or THF (Scheme 1). The reaction progress was monitored by UV−vis and ^{1}H NMR spectroscopy, and the products were separated chromatographically.

The internal carbon atom of the inverted pyrrole in the initial nickel(II) complex of inverted porphyrin **1** has the character of an sp^2 carbanion coordinated to the metal cation. It can be reversibly protonated,[5d,8b,17] which is accompanied by a change of its hybridization to sp^3, and the Ni−C bond is preserved. Although exposed, the external nitrogen should not be a primary alkylation target since it bears proton that is hard to substitute under neutral conditions. It seemed likely that the selectivity for alkylation at the internal carbon would be improved in the absence of a basic catalyst. Under such the conditions, however, the reaction proceeds only for the most reactive iodoalkanes. It takes several days to convert about 50% of the starting complex into alkylated products. Moreover, the selectivity is rather poor since there are comparable amounts of mono- and dialkylated products in the reaction mixture.[19]

Somewhat surprisingly, in all but one case, application of a basic catalyst not only accelerates the reaction but also promotes alkylation with bromo- and chloroalkanes giving apparently better reaction selectivity with respect to the internally monoalkylated products. The reaction should be carried out under anaerobic conditions since **1** is subjected to autoxidation under basic conditions.[8a] The required reaction period varies depending on the haloalkane.

For iodoalkanes such as methyl or ethyl iodide in the presence of a basic catalyst a significant acceleration of the formation reaction of 2,21-dialkylated products can be observed as well. The dimethylated nickel(II) complex **8** was previously generated either by methylation of **1** using methyl iodide at room temperature or by treating the nickel(II) complex of the 2-methylated homologue of inverted porphyrin with MeI.[19,22] In both cases the reaction took about 2 weeks. On the other hand the full conversion of **1** into paramagnetic 2,21-dimethyl derivative is completed after 7 h of reflux of the starting complex with 30-fold excess of MeI in dichloromethane/ethanol solution with a potassium carbonate suspension.

In some cases (e.g. for CH_3Br/K_2CO_3/dibenzo[18]crown-6 in CH_2Cl_2) a considerable amount (about 30% of alkylated product) of 2-methyl-substituted complex[12] **9** is formed, the product that has not been observed in the case of alkylation of **1** with methyl iodide in the absence of a base.[19] It seems to be in line with predicted activation of the external nitrogen toward alkylation by proton scavengers. Likely, the relative reaction rates of the internal and external alkylation depend on the halogen in RX and on the form of the basic catalyst.

As we have reported recently,[23] reaction of **1** with dihalomethanes yields nickel(II) complexes of bis(porphyrinoid) products **10** and **11** (Chart 2). However, in the presence of primary alcohol, e.g. ethanol, monomeric 2- and 21-alkoxymethyl-substituted derivatives (**12** and **13**) are formed instead of dimeric species.[24]

Reaction of **1** with 1,2-dibromoethane yields both dimeric 21,21′-ethylene-linked dimer **14** and 2-bromoethyl-substituted monomer **15**, while alkylation with 1,3-dibromopropane results solely in the formation of the 21-allyl-substituted derivative **16**.[24]

Characterization. The alkylated derivatives of **1** have been characterized by optical spectra, mass spectrometry, and ^{1}H and ^{13}C NMR including 2D homo- and heteronuclear correlation techniques.

In all cases, the apparent molecular ions in the mass spectra agree with the assumed elemental composition having the appropriate *m*/*z* ratio as well as the correct isotope pattern. The UV−vis spectra of monomeric nickel(II) complexes of inverted porphyrin possessing an alkyl bound to the internal carbon of the inverted pyrrole are all similar regardless of the substituents at 21-C.[19,24]

The proton NMR spectra of the monomeric compounds having an alkyl bound to the internal carbon display a typical

(22) Chmielewski, P. J.; Latos-Grażyński, L. *Inorg. Chem.* **2000**, *39*, 5639.
(23) Schmidt, I.; Chmielewski, P. J. *Chem. Commun.* **2002**, 92.
(24) Schmidt, I.; Chmielewski, P. J.; Ciunik, Z. *J. Org. Chem.* **2002**, *67*, 8917.

Chart 2. Monomeric and Dimeric Products of Reaction of **1** with Dihaloalkanes[23,24]

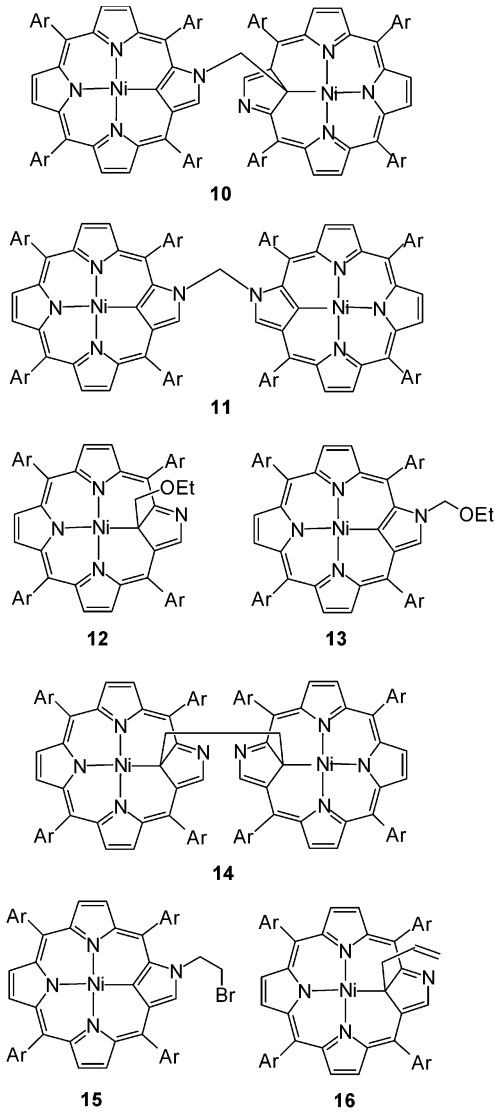

pattern that includes a low-field signal for proton 3 (9.5−9.7 ppm), a set of six pairwise spin−spin-coupled signals of β-pyrrole protons (8.3−8.8 ppm), broad signals of *ortho*-protons (7.9−8.3 ppm at 298 K), and overlapping multiplets for the remaining *meso*-phenyl protons (7.5−7.8 ppm). These features are similar for all these compounds. The most diagnostic for each of these complexes is a high-field region of the spectra (−5 to 1 ppm) where some signals of the alkyl substituents can be found. Their upper-field positions are related to the diatopic current of the carbaporphyrinoid and unequivocally indicate the intraannular location of the substituents (Figure 1). For the benzyl-substituted species the substituent signals are spread over a broader region. The shielding effect of the ring current affects not only methylene but also phenyl protons, according to their distance from the aromatic porphyrin ring. Thus, the *ortho*-protons resonate further upfield (by ∼1.5 ppm) than *meta* and *para* protons.

The molecules are nonplanar which is indicated by the differentiation of the signals for the *ortho*-protons of the *meso*-phenyls that are broad at room temperature due to fast rotation but sharpen at 213 K. The pyramidal hybridization

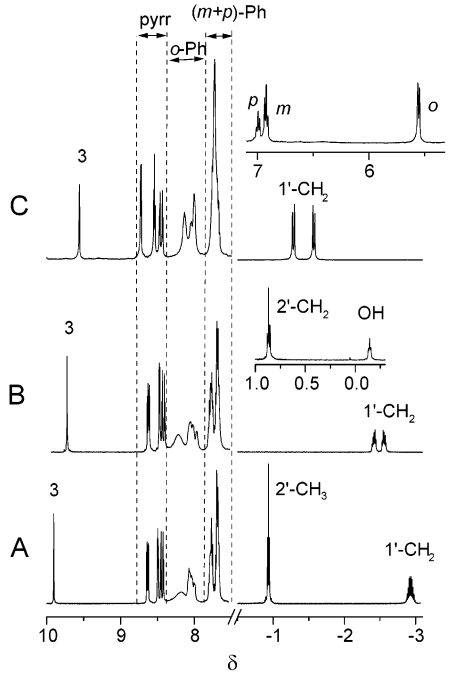

Figure 1. ^{1}H NMR spectra (500 MHz, $CDCl_3$, 298 K) of 21-alkylated nickel(II) complexes of an inverted porphyrin: A, **3**; B, **4**; C, **7**. Assignments: pyrr, β-pyrrole; 3, inverted pyrrole; *o*-, *m*-, *p*-Ph, *ortho*, *meta*, *para* protons of *meso*-phenyls; *o*, *m*, *p*, *ortho*, *meta*, *para* protons of benzyl substituent in **7**; 1′, methylene group attached directly to 21-C.

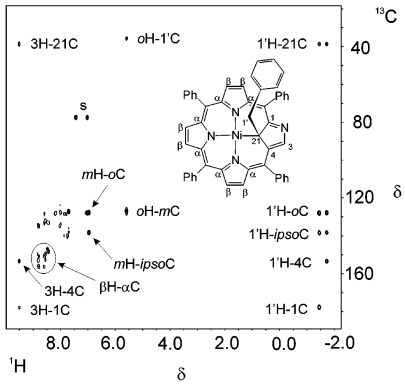

Figure 2. ^{1}H−^{13}C HMBC map of **7** ($CDCl_3$, 223 K). The graph shows assignments of the correlation signals.

of 21-C can be derived from ^{13}C NMR spectra of 21-alkylated nickel complexes of inverted porphyrin where its signal appears in the region of 30−40 ppm that is typical of sp^3 carbons with no proximal heteroatom. It can be easily identified in the ^{1}H−^{13}C HMBC map since it correlates with proton 3 (Figure 2).

Protons of the methylene group directly attached to the inner carbon of the inverted pyrrole are diastereotopic, which reflects the asymmetry of 21-C and the chirality of the molecule. The differentiation can be seen most clearly for the benzyl substituent in **7** (Figure 1C) for which two sharp doublets appear around −1.5 ppm with a coupling constant ^2J = 13.7 Hz. These protons are spin−spin coupled with carbon nuclei of the phenyl ring of the substituent and those of the inverted pyrrole. The coupling constants of 1′-H with 21-C, *ipso*, and *ortho* carbon nuclei seem to be similar for both protons since equally strong correlation peaks with these

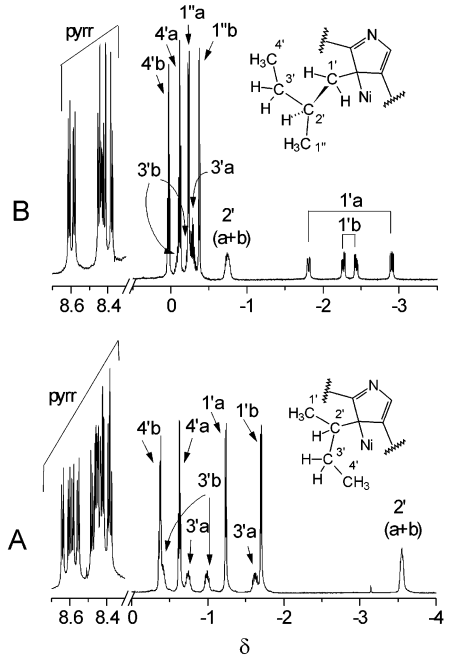

Figure 3. Low- and high-field parts of the ^{1}H NMR spectra (500 MHz, $CDCl_3$, 298 K) of **5** (A) and **6** (B) presenting the occurrence of diastereomers. The graphs show assignments of substituent protons. Labels "a" and "b" differentiate protons of various diastereomers; pyrr = β-pyrrole.

carbons are observed in the HMBC map (Figure 2). However, they differ considerably in the values of $^3J_{HC}$ with 1-C and 4-C. Hence, there is only one correlation instead of two in the HMBC map for each of the latter nuclei with methylene protons 1′. We observe such a behavior for all the other complexes that have a methylene fragment attached to the 21-C. This may indicate restricted rotation around the 1′-21 bond reflecting dependence of a vicinal H−C coupling on the torsional angle.

The alkylation of **1** is nonstereospecific when carried out under the conditions described above. For substituents that contain their own centers of chirality (i.e. *sec*-butyl in **5** and 2-methylbutyl in **6**) the 1:1 mixtures of diastereomers are formed. Their ^{1}H NMR spectra show separate sets of signals for each of the diastereomers, particularly in the high-field region (Figure 3). In the case of **5**, which contains two directly bound asymmetric carbons, there are 12 signals of β-pyrrole protons. A differentiation of chemical shifts and coupling constants between the chemically equivalent protons of the methylene groups is particularly well noticeable for both diastereomers **a** and **b** of **5** and **6**. For compound **6** the diastereomers have different configuration only on 21-C since a pure enantiomer *S* of 2-methylbutyl iodide has been used for its synthesis. Since no racemization is expected for the substituent, any enantiomer excess in the alkylation reaction would appear in ^{1}H NMR as a higher concentration of one of diastereomers.

Previously, we observed the 1:1 mixture of diastereomers (i.e. racemate and a *meso*-form) for "symmetric" dimer **14** containing two chiral carbon atoms linked by the ethylene bridge.[24]

Protonation. Alkylation of 21-C enhances the nucleophilicity of 2-N since it changes its pyrrolic character in **1** into a pyridine-like character in **2**−**7**, **10**, **12**, **14**, and **16**. Thus, protonation of this site is facile. Since such a protonation changes the overall charge of the complex, the presence of a counteranion is required. The counteranion coordinates to the nickel(II) ion changing the geometry of its coordination sphere from square-planar to square-pyramidal (Scheme 2). Consequently, the metal ground state is transferred from singlet to triplet and the complexes become paramagnetic.[19] Coordination of an apical anionic ligand is a consequence of protonation; thus, the character of the five-coordinated complexes is very labile. The ligand exchange as well as deprotonation with restitution of the diamagnetic precursor is facile. In fact, the latter process can be accomplished by addition of water to the solution of the protonated species in dichloromethane or by passing the solution down a silica gel column.

Scheme 2. Protonation of External Nitrogen of Inverted Pyrrole

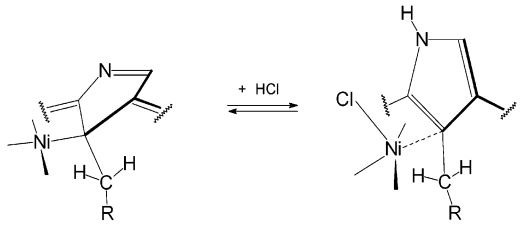

The ^{1}H NMR spectra of the protonated species can be obtained in situ by addition of a solution of acid directly to the NMR tube, which allows the control on concentration of acid and observation of possible consecutive equilibria. An alternative method of sample preparation is dissolution of protonated sample. However, this method limits the concentration of the apical ligand that can lead in some cases to dynamic phenomena related to its coordination and consequently to the broadening of spectral lines. In such cases addition of an excess of anionic ligand in the form of a tetraalkylammonium salt is necessary to saturate the equilibrium. We do so in the case of variable-temperature experiments to eliminate interference of chemical exchange.

The spectra of the 2-protonated−21-alkylated complexes from **2**-HCl to **7**-HCl, **10**-HCl, and **16**-HCl are typical for the paramagnetic pentacoordinated nickel(II) complexes of porphyrin analogues.[2a,19,22,25] The assignment of the signals is based on selective deuteration in all pyrrole positions, application of deuterated acids, and relative line intensities and widths. The spectra consist of widespread, relatively narrow (line half-width < 200 Hz) low-field shifted signals of β-pyrrole protons (20−80 ppm), the high-field-shifted signals of 3-H (−15 to 1 ppm) and 2-NH (−30 to −20 ppm), and aryl proton peaks occurring in the crowded region −10 to 15 ppm (Figure 4, Table 1). These features that are common for all paramagnetic complexes under study result from the spin density delocalization on the macrocyclic

(25) (a) Latos-Grażyński, L. *Inorg. Chem.* **1985**, *24*, 1681. (b) Lisowski, J.; Latos-Grażyński, L.; Szterenberg, L. *Inorg. Chem.* **1992**, *31*, 933. (c) Chmielewski, P. J.; Latos-Grażyński, L. *Inorg. Chem.* **1992**, *31*, 5231. (d) Latos-Grażyński, L.; Pacholska, E.; Chmielewski, P. J.; Olmstead, M. M.; Balch, A. L. *Inorg. Chem.* **1996**, *35*, 566. (e) Chmielewski, P. J.; Latos-Grażyński, L.; Olmstead, M. M. Balch, A. L. *Chem.—Eur. J.* **1997**, *3*, 182.

Table 1. ^{1}H NMR Data for Paramagnetic Nickel(II) Complexes of 2-Protonated−21-Alkylated Inverted Porphyrin in $CDCl_3$

complex (temp, K)	β-pyrrole	3-H	2-NH	R	*meso*-phenyl and other paramagnetically shifted protons
4-HCl (298)	57.2, 56.6, 49.9, 46.4, 26.2, 24.8	−2.2	−22.7	90.1, 50.9 (1′)	11.2, 10.5, 10.1, 10.0, 9.2, 9.0, 8.8, 8.6, 6.9, 6.7, 6.5, 5.1, 4.7, 3.0
4-HCl (213)	78.5, 78.0, 68.1, 62.8, 35.5, 33.8	−6.3	−38.2	140.3, 60.4 (1′), −0.2, −2.1	13.2, 12.1, 11.6, 11.2, 10.1, 10.0, 9.4, 8.5, 6.3, 5.7, 3.5, 2.9
5-HCl (298)	(58.8, 55.7, 48.3, 46.5),[a] (58.3, 56.2, 50.4, 45.0),[b] 29.6, 29.4, 29.0, 28.9	-6.1	(−21.5)[b] (−22.2)[a]	124.4, 105.9 (2′), 15.7 (3′)	10.5, 10.0, 9.4, 9.0, 8.6, 8.3, 5.7, 4.2, 3.7
5-HCl (213)	(80.7, 76.2, 65.5, 63.2, 41.1, 39.5),[a] (80.0, 76.8, 69.1, 60.5, 40.2, 39.2)[b]	−13.7	(−37.0)[c]	189.6, 128.4 (2′), 31.9 (3′), −1.4, −2.7	16.7,12.9, 12.5, 11.9, 11.7, 11.5, 10.7, 10.0, 9.7, 9.5, 9.3, 9.0, 8.5, 8.2, 8.1, 6.7, 6.2, 6.0, 4.4, 4.2, 3.9, 3.2, 2.9, 2.3
6-HCl (298 K)	57.1, 56.9, 56.8, 56.7, 50.9, 50.5, 46.9, 46.6, 27.2, 26.7, 25.6, 24.9	−1.5, −1.8	(−22.6)[c]	120.0, 89.5, 64.0, 31.4 (1′), 0.4, −1.8 (CH_3), −4.7 (CH_2)	11.2, 10.6, 10.5, 10.3, 9.3, 9.2, 9.0, 8.7, 7.9, 6.9, 6.8, 4.3, 4.1, 3.7, 0.9
6-HCl (213)	78.0, 77.9, 77.8, 77.5, 69.6, 69.1 63.3, 62.8, 36.7, 36.1, 34.5, 33.7	−3.5, −4.4	(−38.1)[c]	191.2, 161.1, 57.1, 26.2 (1′), −0.5, −2.8 (CH_3), −7.2 (CH_2)	13.2, 12.6, 12.2, 11.9, 11.8, 11.7, 11.0, 10.3, 10.0, 9.9, 9.6, 9.2, 8.5, 7.7,6.4, 5.5, 3.5, 2.0, 1.8, 0.5
7-HCl (298)	56.9, 56.3, 50.6, 46.6, 26.0, 24.3	1.1	−24.2	94.5, 47.3 (1′)	11.3, 10.6, 10.4, 10.3, 10.0, 9.3, 8.8, 8.7, 6.9, 6.4, 5.5, 5.0, 4.7, 4.3, 4.1
7-HCl (213)	78.9, 78.8, 69.7, 63.8, 35.6, 33.3	−0.9	−40.4	150.3, 51.1 (1′)	13.4, 12.2, 11.8, 10.9, 10.1, 9.7, 9.2, 8.8, 6.2, 5.5, 4.5, 3.3, 2.5, 0.6
16-HCl (298)	57.0, 56.5, 50.2, 46.6, 26.1, 24.6	0.9	−23.0	87.6, 55.3 (1′) 16.9 (2′)	11.1, 10.4, 10.0, 9.2, 8.9, 8.7, 8.6, 6.9, 6.5, 6.1, 6.0, 5.3, 4.8, 4.3, 4.2, 3.8
16-HCl (213)	78.2, 77.8, 68.5, 62.9, 35.3, 33.5	−1.2	−38.2	136.1, 69.1 (1′) 23.1 (2′), 14.7 (3′)	13.2, 12.1, 11.6, 10.0, 9.6, 7.8, 6.2, 5.6, 3.6, 2.8
2-HCl (293)[d]	58.1, 58.1, 52.4, 48.2, 26.5, 24.9	2.0	−23.1	109.7	11.3, 10.7, 10.5, 10.4, 9.3, 9.2, 8.7, 7.8, 6.9, 6.4, 5.1, 4.9, 4.1

[a] Signals of diastereomer **a**. [b] Signals of diastereomer **b**. [c] The same chemical shift for both diastereomers. [d] Data from ref 19.

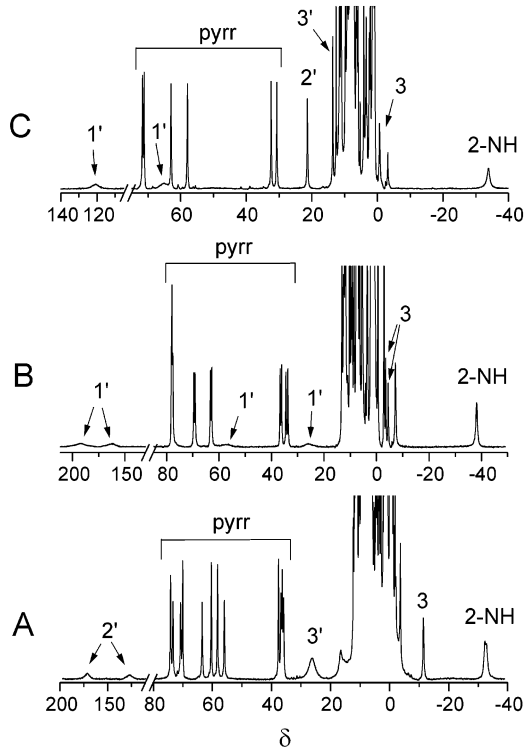

Figure 4. ^{1}H NMR (500 MHz, $CDCl_3$) of **5**-HCl (A, 233 K), **6**-HCl (B, 213 K), and **16**-HCl (C, 233 K). Assignments are as in Figures 1−3.

ligand in which σ-orbitals are predominantly involved causing a low-field shift of β-pyrrole signals. Some contribution of the π-type orbitals in the spin density transfer results in differentiation of isotropic shift of these signals and determines the upfield position of 3-H and 2-NH signals. For the latter protons the overlap of π-symmetry orbitals of metal and ligand is effective due to a tilt of the inverted pyrrole out of plane of the macrocycle.[19,22] The substituent protons attached to the carbon that is directly bound to the 21-C (assigned 1′ but 2′ in the case of **5**-HCl) give considerably broader signals, which reflect their closeness to the paramagnetic center. The protons of the methylene groups are diastereotopic, and the difference in their chemical shifts reaches several tens up to more than a hundred ppm. Protons located on the carbons that are further from 21-C (more than two bonds) give less paramagnetically shifted signals. For **5**-HCl the methylene group of the secondary butyl substituent (3′) has a significant downfield shift. In **16**-HCl proton 2′ of the allyl substituent resonates at 16.9 ppm (298 K, $CDCl_3$). Similarly, in the case of paramagnetic unsymmetrical dimer **10**-HCl only one pyrrole proton of the *N*-substituted fragment (most likely proton 3, which is the closest to the methylene linker) shows a paramagnetic shift comparable to those of β-pyrrole protons of C-substituted subunits.[23]

Diastereomers are observed for the complexes **5**-HCl and **6**-HCl containing substituents with their own chiral centers. The chemical shifts of pyrrole protons are particularly differentiated for the diastereomers of **5**-HCl having a secondary butyl group attached to the internal carbon of the

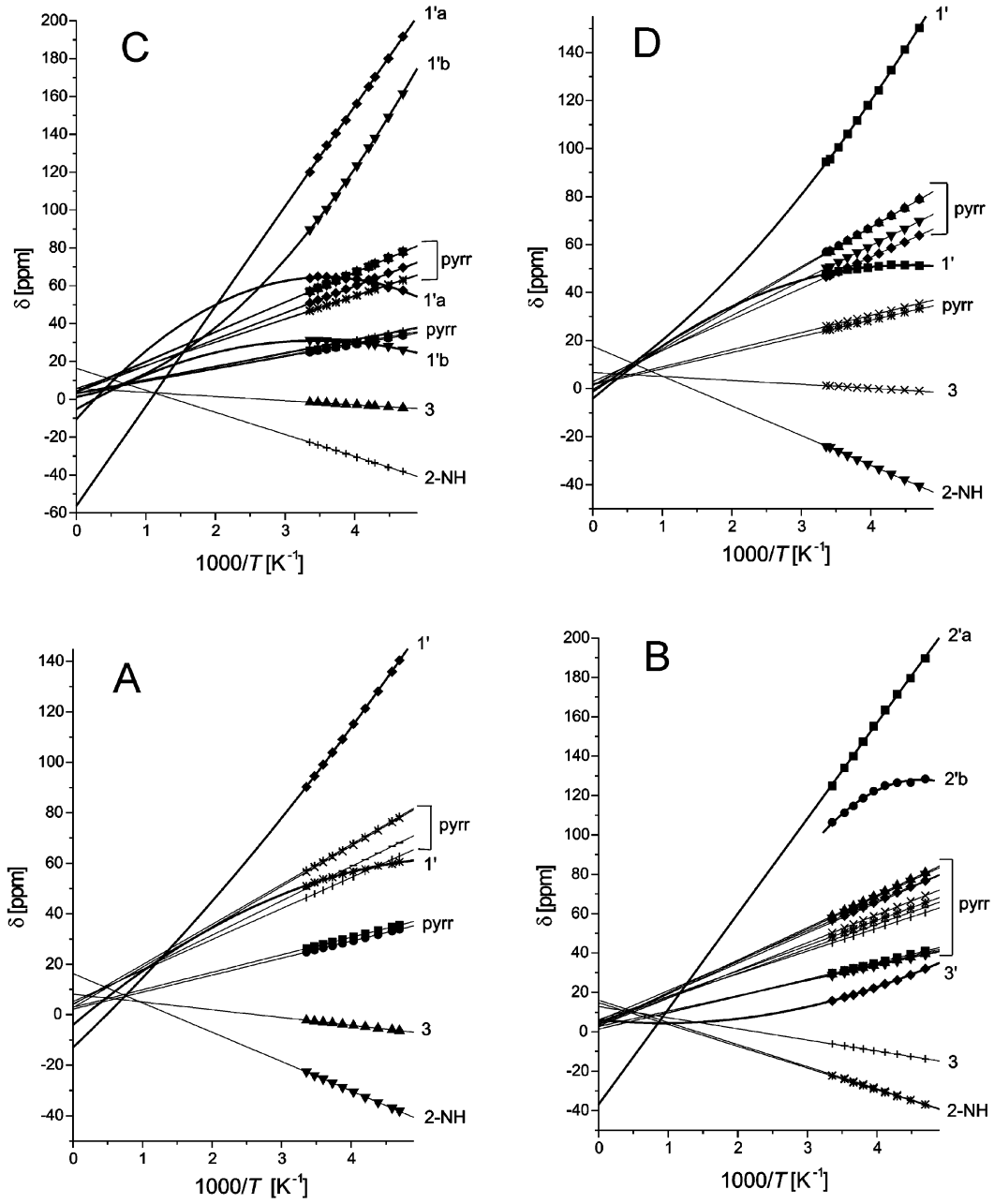

Figure 5. Curie plots of **4**-HCl (A), **5**-HCl (B), **6**-HCl (C), and **7**-HCl (D) based on the data taken for $CDCl_3$ solutions of respective systems. The assignments "a" and "b" are introduced to distinguish the diastereomers but are not related to labeling of the diamagnetic precursors in Figure 3. The nonlinear dependencies have been traced by means of a second-order polynomial fitting procedure but are drawn only to join the experimental points.

inverted pyrrole. Moreover, for this complex the signals of isomers differ also in line widths and in the integral signal intensities indicating about 20% excess of one of them in the temperature range 273−233 K in $CDCl_3$ (Figure 4A). At 213 K concentrations of both diastereomers are equal. Since the mixture of their diamagnetic precursors contained exactly the same concentrations of both diastereomers (Figure 3), the observed diastereoselectivity reflects different susceptibility of nickel(II) to apical ligation of chloride upon protonation of 2-N in the stereoisomers. It results from the different steric factors in the proximity of coordination center in the diastereomers since the electronic substituent effect is the same in both complexes. There is also a significant difference (about 45 ppm at 233 K) in chemical shifts of the protons 2′, i.e., those attached to the secondary carbon that is directly bound to the 21-C. It may reflect an influence of the preferred orientation of alkyl group on the contribution of π-spin density delocalization to the isotropic shift.[26]

Deviation from planarity causes a considerable spin density transfer from the metal to the inverted pyrrole via a π-orbital framework and, consequently, the more upfield paramagnetic shift of protons 3 and 2-NH. However, protons of the alkyl groups attached directly to the ring, onto which spin density is delocalized predominantly by the π-mechanism, display a low-field shift.[26] Spin density transfer via a σ-orbital

(26) Walker, F. A.; Simonis, U. In *Biological Magnetic Resonance, Vol. 12: NMR of Paramagnetic Molecules*; Berliner, L. J., Reuben, J., Eds.; Plenum Press: New York, 1993; p 133.

framework always gives a positive contribution to the isotropic shift (low-field shifting) that attenuates as the number of bonds between the paramagnetic metal center and the given nucleus increases.[26] Hence, in the case of protons bound to the carbon attached to 21-C both σ- and π-contributions to the isotropic shift are positive. Since these protons are the least distant from the metal ion (3 bonds), their signals are expected to be the most downfield-shifted among all protons in the molecule. Indeed, for the complexes where no diastereotopic differentiation of protons is observed, such as **2**-HCl[19] or **5**-HCl the signals of methyl protons or 2′-H, respectively, are very strongly paramagnetically shifted to the low field (δ > 100 ppm). On the other hand, for the complexes with diastereotopic methylene bound to 21-C (**4**-HCl, **6**-HCl, **7**-HCl, **10**-HCl,[23] **16**-HCl), one of the CH_2 protons is much less downfield shifted than the other and even less shifted than signals of some of the more distant (4 bonds) β-pyrrole protons. For example, in the case of **7**-HCl the difference of chemical shifts between methylene protons of the benzyl group reaches 100 ppm (213 K, $CDCl_3$). This observation can be accounted for by a contribution of the dipolar mechanism to spin delocalization onto these parts of the molecule that are closest to the paramagnetic center.[25] The variable-temperature ^{1}H NMR experiments support such an interpretation. Dependencies of δ vs $1/T$ (Figure 5) for pyrrole protons are linear with extrapolated intercepts in most cases only moderately deviated (by 1−5 ppm) from the values predicted on the basis of chemical shifts of diamagnetic references (i.e. unprotonated diamagnetic complexes for pyrrole and alkyl protons, monocation of inverted porphyrin[5a] for 2-NH). On the other hand, for the alkyl protons 1′ (2′ in the case of **5**-HCl) these dependencies are either nonlinear or have intercepts very strongly deviating from those expected. In one case (**6**-HCl), reverse temperature dependencies of chemical shift are observed for two out of four methylene protons 1′ of the diastereomers. The difference in paramagnetic shifts and in the temperature dependencies between the protons belonging to the same methylene group can arise from their different mean orientation with respect to the principal axes of the magnetic susceptibility tensor. In other words, the geometric factor that governs the sign and value of the dipolar component of the isotropic shift is responsible for the differentiation of chemical shift of these diastereotopic protons 1′.[27]

As we[8b,17,24] and others[5d] reported recently, protonation of the internal carbon of the inverted pyrrole in nickel(II) complexes of 21-unsubstituted inverted porphyrins results in a distribution of the additional positive charge within the molecule different from that observed in the paramagnetic species described above. Consequently, nickel(II) ion remains four-coordinated and diamagnetic despite analogous changes of charge that take place upon protonation. It can be accounted for by the bulkiness of the substituent bound to the internal carbon in 21-C-alkylated complexes that may facilitate displacement of the metal ion from the plane

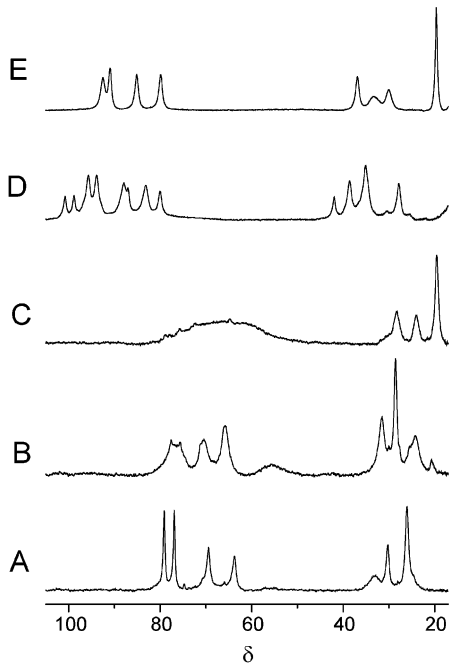

Figure 6. Low-field part of the selected ^{1}H NMR spectra (500 MHz, CD_2Cl_2) taken in the course of titration of **10** with TFAD: A, 1 equiv of acid, 213 K; B, 2 equiv of acid, 213 K; C, 4 equiv of acid, 213 K; D, 4 equiv of acid 173 K; E, as in D + 2 equiv of $[BzEt_3N]Cl$.

defined by the $N_3C(R)$ chromophore and coordination of an apical anionic ligand. If H^+ is attached to the internal carbon, the charge of the proton is delocalized onto the external nitrogen.

Asymmetric dimer **10** contains both types of potential protonation targets, i.e., external nitrogen and internal carbon. Addition of either TFAH or HCl[23] effectively converts the complex into the paramagnetic species **10**-HX due to protonation of the external nitrogen of the 21′-substituted fragment. In the case of HCl, the increase of its concentration does not change the number of spectral lines or their positions in the ^{1}H NMR spectrum either at room temperature or at 213 K. It suggests that in the case of hydrochloric acid only one protonation site is involved. On the other hand, the spectrum depends on the acid concentration when TFAH is used for titration of **10** at low temperatures. Addition of 1 equiv of acid at 213 K results in a spectrum consisting of six downfield-shifted β-pyrrole peaks of C-substituted fragment and one signal of pyrrole proton of N-substituted subunit of the dimer (Figure 6A). Further increase of acid concentration causes considerable broadening of the spectral lines. At 173 K in CD_2Cl_2 the lines sharpen up and double in number due to a slowing down of the chemical exchange (Figure 6D). By exploitation of the kinetic isotope effect, the chemical exchange can be more effectively slowed when deuterated trifluoroacetic acid (TFAD) is applied. The number of peaks does not change any more with increasing concentration of acid (up to 10-fold excess). This behavior can be accounted for by a protonation of 21-C in the N-substituted fragment of the complex and formation of the diprotonated species [(**10**-TFAH)H]TFA (Scheme 3). The doubling of the number of pyrrole signals likely reflects presence of diastereomers due to the occurrence of two

(27) Jesson, J. P. In *NMR of Paramagnetic Molecules*; La Mar, G. N., Horrocks, W. D., Holm, R. H., Eds.; Academic Press: New York, 1973; p 1.

Scheme 3. Protonation and Demetalation of Asymmetric Dimer **10**

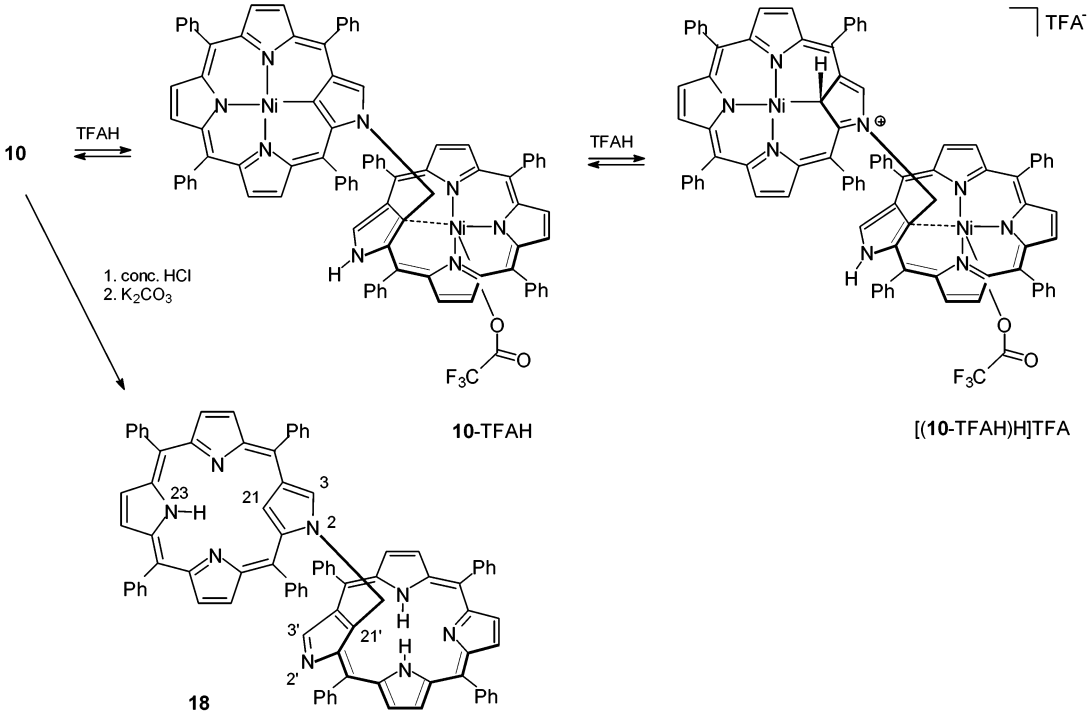

different stereogenic centers: the one that has a permanent character is combined with C-subsituted fragment while the other is induced by protonation of 21-C of N-substituted subunit of the dimer. Alternatively, formation of a tight ion pair between the C-protonated fragment of the diprotonated species and TFA^- can be accounted for the presence of two species at higher acid concentration. Addition of 2-fold excess of benzyltriethylammonium chloride to the sample solution apparently converts the diprotonated complex to monoprotonated since there is only one set of pyrrole signals observed in the ^1H NMR spectrum (Figure 6E). Also spectrophotometric titration of **10** with TFAH at room temperature shows consecutive formation of two species whose relative concentration depends on the amount of acid. The first protonated species is formed at relatively low concentration of TFAH, thus, it can be formulated as a monoprotonated complex **10**-TFAH, while the second form, dominating at much higher acid concentrations (over 6 equiv), should be assigned to the diprotonated complex (Figure 7). Further addition of acid leads to the protonation of internal coordination core of the macrocycle that is combined with demetalation.

Demetalation and Dealkylation. Free ligands of 21-alkylated inverted porphyrins can be obtained by acidification of their solution with concentrated acids and neutralization of the initially formed cations. The ^1H NMR spectrum of 5,10,15,20-tetraphenyl-21-benzyl-2-aza-21-carbaporphyrin (**17**) shows features indicating nonplanarity of the ligand, e.g. differentiation of *ortho* protons of *meso*-phenyls and diastereotopic methylene protons of the 21-benzyl substituent (-3.53, -3.59 ppm, $^2J = 16.5$ Hz, 298 K, $CDCl_3$). The 21-C adopts an sp^2 hybridization in the free ligand which can be inferred from the position of its signal in the ^{13}C NMR spectrum (106.6 ppm). Significantly, the signal of 3-H is shifted considerably upfield (almost 3 ppm) with respect to its position in **7**. This indicates a change in the π-electron density delocalization path causing less effective deshielding of the external part of the inverted pyrrole by the ring current (Chart 3).

Similarly, in the case of the 2,21′-CH_2-linked diporphyrin **18** (Scheme 3), despite the lack of an asymmetric carbon atom, the methylene protons are still diastereotopic due to

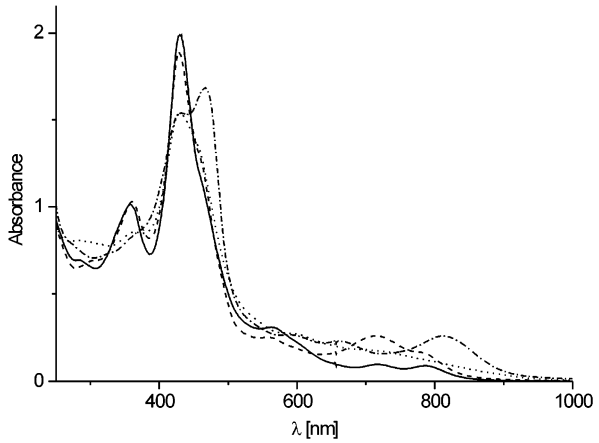

Figure 7. Selected optical spectra (CH_2Cl_2, 295 K) taken in the course of titration of **10** with TFAH: solid line, 0 equiv; dashed line, 1.5 equiv; dotted line, 10 equiv; dash−dotted line, 150 equiv.

Chart 3. Delocalization Paths in **7** and **17**

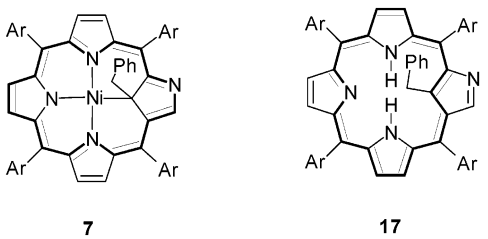

Scheme 4. Demetalation and Dealkylation of **7**

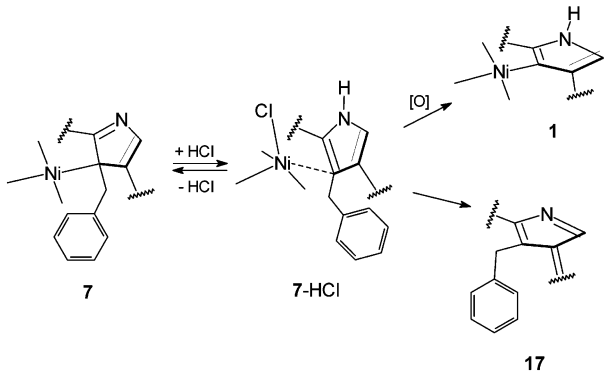

the nonplanar geometry of the whole molecule. In a ^{1}H NMR spectrum of this compound ($CDCl_3$, 233 K) the linker protons are represented by an AB system (−2.42, −2.75 ppm, ^2J = 16.0 Hz) resonating at noticeably higher field than the bis-(nickel(II)) complex **10** (0.11, −0.47 ppm, ^2J = 15.6 Hz).[23] The dimeric and asymmetric character of **18** is reflected by the number of distinct signals for the pyrrole protons. There are 12 β-pyrrole proton signals that can be assigned in the spectrum on the basis of a COSY experiment. Two singlets, those of proton 3 (5.65 ppm) and 3′ (6.71 ppm), are also shifted to the higher field with respect to those in **10** (6.71 and 9.35 ppm, respectively). Proton 3 is spin−spin coupled with proton 21-CH, which gives a signal at 0.15 ppm. The 23-NH proton with a signal at 3.16 ppm correlates in the COSY map with two pyrrole protons which give a complex signal at 7.68 ppm. Two internal NH protons of the C-substituted fragment of the dimer show a relatively broad signal at −3.30 ppm. Thus, diporphyrin **18** possesses two different potentially dianionic coordination centers. Ring current effect of these two aromatic systems affects chemical shifts of some protons. In particular, protons of one of the *meso*-phenyl show high-field shifts (5.58−6.61 ppm) with respect to their usual positions. Moreover, these five protons give distinct signals regardless of the temperature (213−323 K), which indicate that rotation of this phenyl ring is strongly restricted by the vicinity of a bulk substituent constituted by the other porphyrin subunit.

In most cases, if protonation take place only on the external nitrogen, full recovery of the starting diamagnetic alkylated complexes is possible even for the long stored solutions of the protonated species. However, in the case of **7**-HCl, **12**-HCl, and **16**-HCl a competitive dealkylation process takes place. About 80% of **7** is converted to complex **1** (Scheme 4) after 2 h in refluxing DMF with an admixture of a dry gaseous HCl. After a few days, dealkylation of **7**, **12**, and **16** can be observed at room temperature in chloroform or dichloromethane solutions in the presence of acid. During the period of 5 days of standing on the benchtop in a $CDCl_3$ solution more than 85% of **7**-HCl loses its 21-C substituent yielding **1**. Such a conversion requires breaking a bond between 21-C and 1-C′.

There are several reports concerning C−C bond activation in solution of organometallic compounds mostly containing late transition elements of the second and third row.[28] Detailed study on the dealkylation of *N*-alkylated regular porphyrins has been performed by Lavalee and co-workers.[21,29] The nucleophilic displacement of *N*-substituent was shown to be effective for various complexes of divalent transition metals ions. Stabilization of intermediate carbocation in the case of benzyl group evidently promoted dealkylation which is in line with the S_N1 character of that process.[29]

In the case of **7**, dealkylation of the protonated species is driven by oxidation. In fact, we observe characteristic signals of benzaldehyde (10.01 ppm, CHO group; 7.87, 7.62, 7.52 ppm, *ortho*-, *para*-, and *meta*-protons, respectively) together with signals of **1** in the ^{1}H NMR spectrum of the solution that initially contained **7**-HCl. Significantly, there is no such dealkylation observed for **7**-HCl when its solution is prepared and stored in strictly anaerobic conditions. Evidently, nickel(II) ion and acid contributions are both necessary to accomplish that oxidative dealkylation since free ligand **17** is stable in acidic conditions in the presence of air and so is the unprotonated complex **7**. The C−C bond-breaking process seems to be dependent on the character of the substituent. It is promoted by allylic/benzylic functionality or strong electron-donating alkoxy group.

Redox Properties. Due to the potentially trianionic coordination core the unsubstituted inverted porphyrin is expected to stabilize higher oxidation states of the transition metals.[8a−d] Alkylation of either external nitrogen or internal carbon of the inverted pyrrole reduce the accessible negative charge that may be introduced by a macrocyclic ligand from −3 to −2. In fact, oxidation of **1** takes place without deprotonation of the external nitrogen and, thus, an additional anionic ligand is required[8a] to neutralize the positive charge since the macrocycle remains bis-anionic. In the case of nickel(II) complexes of inverted porphyrin and its externally methylated derivative the first oxidation is observed at potentials below 800 mV suggesting that the metal ion rather than the ligand is oxidized.[8a−c] As expected, strong bases (e.g. potassium *tert*-butoxide) capable of removing the 2-NH proton[24] considerably change the oxidation potential of the complex shifting about 400 mV to the less positive values (Table 2, $[\mathbf{1}]^-$). On the other hand, addition of acids that can protonate the complex on 21-C have little or no effect on the potential of Ni^{II}/Ni^{III} couple (Table 2, **1**-TFAH).

Cyclic voltammograms for the 21-alkylated nickel(II) complexes of inverted porphyrin were recorded in CH_2Cl_2 solution with 0.1 M tetrabutylammonium perchlorate (TBAP) as a supporting electrolyte and Ag/AgCl reference electrode at room temperature. When being scanned into the positive potentials, a typical voltammogram (Figure 8A) consists of an irreversible or quasi-reversible couple (1) in the range of

(28) For a comprehensive review of C−C bond activation by metal complexes in solution, see: Milstein, D.; Rybtchinski, B. *Angew. Chem., Int. Ed.* **1999**, *38*, 870.

(29) (a) Lavalee, D. K. *Inorg. Chem.* **1976**, *15*, 691. (b) Lavalee, D. K. *Inorg. Chem.* **1977**, *16*, 955. (c) Kuila, D.; Lavalee, D. K. *Inorg. Chem.* **1983**, *22*, 1095. (d) Lavalee, D. K.; Kuila, D. *Inorg. Chem.* **1983**, *22*, 3987. (e) Doi, J. D.; Compito-Magliozzo, C.; Lavalee, D. K. *Inorg. Chem.* **1984**, *23*, 79.

Table 2. Cyclovoltammetric Potentials[a] of Nickel(II) Complexes of Inverted Porphyrins in Dichloromethane

complex	$E_a(1)$	$E_c(1)$	$E_a(2)$	$E_c(2)$	$E_a(3)$	$E_c(3)$	$E_a(4)$	$E_c(4)$
1	742	670	1120	932				−1088
1-TFAH	750	674	1120		−442	−522		
$[\mathbf{1}]^-$	344	256						
2	738	588	939				−900	−968
2-TFAH	780	682			−378	−442		−880
4	646	488	1200	1093			−856	−940
4-TFAH	712	592	1330	1120	−383	−446	−806	−980
5	760	522					−894	−980
5-TFAH	820	660			−368	−452	−836	−1026
7	770	527						−940
7-TFAH	782	656			−335	−431		−968
10	756, 896	684, 824	1146					−825
10-TFAH	808, 898	720	1074	908		−292		
11	820, 934	733, 856	1156	1069				−950
12	661	511	1279	1190			−878	−950
12-TFAH	733	646	1453	1135	−370	−448		−864

[a] All potentials (in mV) vs Ag/AgCl.

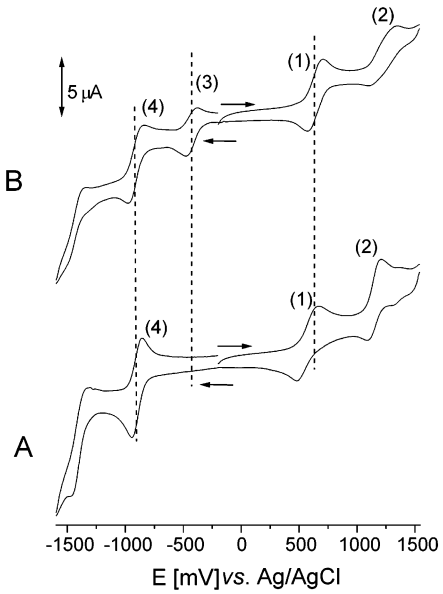

Figure 8. Cyclic voltammograms of **4** (A) and **4**-TFAH (B, 2 equiv of TFAH) in CH_2Cl_2 solutions (supporting electrolyte, 0.1 M TBAP; working electrode, glassy carbon disk; reference electrode, Ag/AgCl; auxiliary electrode, platinum wire; scan rate, 50 mV s^{-1}).

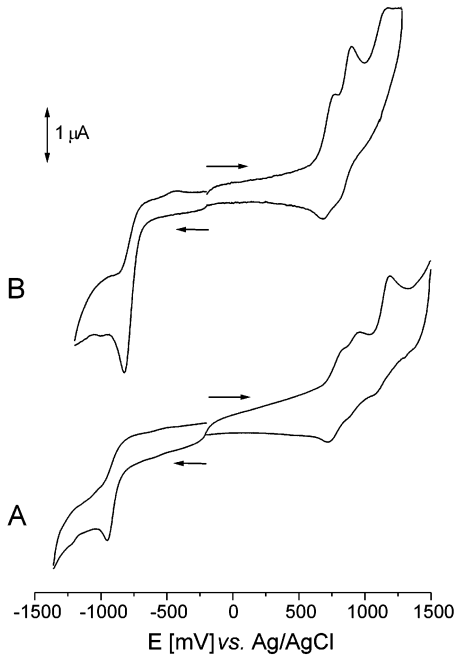

Figure 9. Cyclic voltammograms of **10** (A) and **11** (B) in CH_2Cl_2 solutions (supporting electrolyte, 0.1 M TBAP; working electrode, glassy carbon disk; reference electrode, Ag/AgCl; auxiliary electrode, platinum wire; scan rate, 50 mV s^{-1}).

520−770 mV that can be assigned to the Ni^{II}/Ni^{III} process and irreversible anodic wave (2) at the potentials over 1000 mV combined with oxidation of the ligand. On the negative side, a well-defined quasi-reversible wave (4) at about −900 mV is observed which can be linked with a reduction process of the aromatic macrocycle. The data for the representative examples are collected in Table 2. For the monomeric complexes containing methyl, *sec*-butyl, or benzyl substituents (**2**, **5**, and **7** in Table 2), the first oxidation potentials do not differ considerably from that of the starting complex **1**. Significantly lower potentials (by about 100 mV) are observed for the complexes with substituents containing oxygen, i.e., 2′-hydroxyethyl (**4**) and ethoxymethyl (**12**), that suggest some inductive effect of the heteroatom.

Protonation with TFAH shifts potentials of anodic waves of the first oxidation to the higher values (by 10−70 mV). The alteration of potentials of cathodic peaks for this redox process is more pronounced (by 110−140 mV). Higher potentials reflect lower stability of the nickel(III) ion in protonated species but do not seem to preclude oxidation of the high-spin metal center. The values of these potentials are close to that of complex **1** which can be oxidized chemically by various oxidants to the nickel(III) species.[8a] On the other hand protonation promotes the reduction of the metal ion. A reversible couple (3) at about −400 mV, which is observed after addition of acid for all monomeric complexes under study, can be assigned to the Ni^{II}/Ni^{I} redox process (Figure 8B).

For both dimeric complexes with methylene linker the oxidation pattern is more complicated indicating an interaction between the redox centers (Figure 9). For **10** there are two anodic waves in the range of 750−900 mV of two consecutive oxidations of different parts of the asymmetrical dimer.[23] A similar pattern is observed for the symmetrical 2,2′-CH_2-linked dimer **11**. The stepwise oxidation of porphyrin subunits in **10** and **11** implies an interaction between

Table 3. EPR Data of 21-Alkylated Nickel(III) Complexes of Inverted Porphyrins in Dichloromethane/Toluene Solution[a]

complex	g_x	g_y	g_z	A_x[b]	A_y	A_z[a]	g_{iso}	A_{iso}[b]
4-Cl	2.407	2.173	2.048	c	c	25	2.207	c
7-I	2.305	2.127	2.040	60	80	163	2.169	74
7-Br	2.360	2.146	2.052	30	40	124	2.168	59
7-Cl	2.407	2.175	2.054	c	c	25	2.207	c
7-I(TFAH)	2.290	2.125	2.058	60	75	148	2.159	c
7-H$(TFA)_2$	2.425	2.244	2.082				2.250	
10-I	2.290	2.120	2.040	55	80	160	2.168	74
10-Cl	2.410	2.198	2.062	c	c	28	2.208	c

[a] Frozen solution spectra were taken at 77 K; isotropic spectra were recorded at 298 K. [b] Tensor components (in gauss) of hyperfine coupling with one ^{127}I, ^{79,81}Br, or ^{35,37}Cl nucleus, respectively. [c] Not resolved.

them resulting in modification of redox properties of the second center upon oxidation of the first subunit. Observation of only one two-electron oxidation process is expected for the system containing two identical and noninteracting porphyrin centers.[30]

According to cyclovoltammetric data chemical oxidation of the 21-alkylated nickel(II) complexes of inverted porphyrin should be as effective as oxidation of the starting complex **1**.[8a] Indeed, addition of iodine to a dichloromethane/toluene solution of one of the complexes resulted in observation of an EPR spectrum which can be attributed to nickel(III) species on the basis of the considerable anisotropy of the Zeeman tensor (Table 3).[31,32] Observation of hyperfine coupling with one ^{127}I nucleus (nuclear spin $I = 5/2$) reveals coordination of one iodide ligand to the d^7 metal ion. Moreover, relation of principal components of tensors **g** and **A**(^{127}I) allows one to determine the d_{z^2} orbital as the major metal contribution to the single occupied molecular orbital. In such a case the lowest *g*-value (g_z) should be close to that of free electron (2.0023) and the hyperfine splitting due to an apical ligand A_z should be the largest.

The anionic ligand can be exchanged by addition of an appropriate tetraalkylammonium salt, e.g. bromide or chloride (Figure 10). The spectra closely resemble those obtained by van Koten and co-workers for the nickel(III) complexes of the "pincer" NCN′ ligand.[33] In each case hyperfine splitting indicates the presence of one anionic ligand in the first coordination sphere of Ni^{III}. Acidification of the solution of **7**-I with 1 equiv of TFAH resulted in small but noticeable changes in spin-Hamiltonian parameters (**7**-I(TFAH), Table 3) preserving the general pattern of the spectrum, in particular, showing coordination of one apical iodide ligand. This alteration of parameters can be due to protonation of the external nitrogen of the inverted pyrrole, which takes

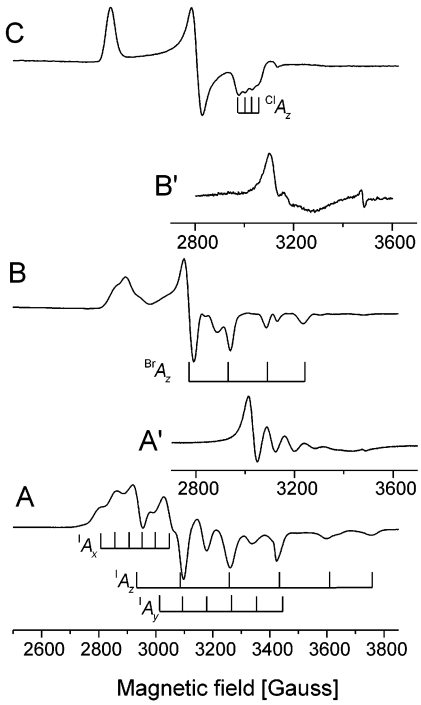

Figure 10. EPR spectra of oxidized complex **7** with various apical ligands in toluene/dichloromethane solution (30/70 v/v): A, **7**-I, 77 K; A′, 298 K; B, **7**-Br, 77 K; B′, 298 K; C, **7**-Cl, 77 K. The resolved hyperfine splittings due to ^{127}I, ^{79,81}Br, or ^{35,37}Cl in anisotropic spectra are marked. Conditions: microwave frequency, $\nu = 9.573$ GHz for anisotropic spectra and 9.782 GHz for isotropic spectra; microwave power, 12.5 mW; modulation amplitude, 8 G; modulation frequency, 100 kHz.

place without ligand exchange. It seems that the considerable steric constraints caused by alkylation of 21-C preclude axial coordination of two ligands. Consequently, it may be anticipated that protonation of the external nitrogen is accompanied by introduction of an additional anion into the second coordination sphere. Addition of 4 equiv of TFAH to the solution of the iodine-oxidized complex changes the EPR spectrum that no longer indicates the presence of an iodide ligand (**7**-H$(TFA)_2$, Table 3). The difference in Zeeman tensor parameters and lack of hyperfine splitting suggest in this case protonation of 2-N with concurrent exchange of ligand coordinating to nickel(III) center. However, solely on the basis of the EPR spectra, we cannot make a definitive conclusion concerning stoichiometry of the oxidized species formed upon addition of acid.

The asymmetric dimer **10** upon addition of iodine gave an EPR spectrum that is very similar to those obtained for monomeric complexes (Table 3). It suggests that only one out of two different nickel(II) centers is oxidized by means of this oxidant.

An attempt on isolation of any of the oxidized species failed likely due to facile reduction of the nickel ion[8a] and some decomposition processes that are linked to the oxidation of the ligand.[34] It should be noted that to date the only stable and structurally characterized organometallic nickel(III) systems, i.e., arenium "pincer" complexes, have oxidation potentials about 500 mV lower[33b] than those of nickel complexes of inverted porphyrin derivatives.

(30) Becker, Y.; Dolphin, D.; Paine, J. B.; Wijesekera, T. *J. Electroanal. Chem.* **1984**, *164*, 335.
(31) Busch, D. H. *Acc. Chem. Res.* **1978**, *11*, 392.
(32) (a) Margerum, D. W.; Anlinker, S. L. In *The Bioinorganic Chemistry of Nickel*; Lancaster, J. R., Jr., Ed.; VCH Publishers Inc.: Weinheim, Germany, 1988; p 29. (b) Salerno, J. C. In *The Bioinorganic Chemistry of Nickel*; Lancaster, J. R., Jr., Ed.; VCH Publishers Inc.: Weinheim, Germany, 1988; p 53. (c) Moura, J. G.; Teixeira, M.; Moura, I.; LeGall, J. In *The Bioinorganic Chemistry of Nickel*; Lancaster, J. R., Jr., Ed.; VCH Publishers Inc.: Weinheim, Germany, 1988; p 191.
(33) (a) Grove, M. D.; van Koten, G.; Zoet, R. *J. Am. Chem. Soc.* **1983**, *105*, 1379. (b) Grove, M. D.; van Koten, G.; Mul, P.; Zoet, R.; van der Linden, J. G. M.; Legters, J.; Schmitz, J. E. J.; Murral, N. W.; Welch, A. J. *Inorg. Chem.* **1988**, *27*, 2466.
(34) Furuta, H.; Maeda, H.; Osuka, A. *Org. Lett.* **2002**, *4*, 181.

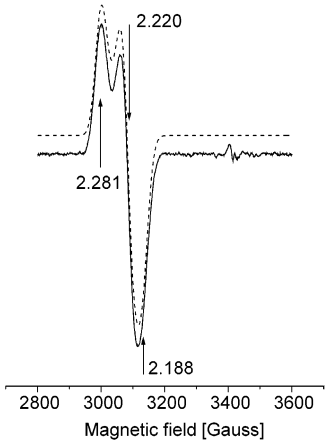

Figure 11. EPR spectrum (solid line) of a species obtained in the reaction of toluene solution of **7** with aqueous hydrazine dihydrochloride. The simulated spectrum (dashed line) was calculated with the spin-Hamiltonian parameters marked. Conditions: microwave frequency, $\nu = 9.5779$ GHz; microwave power, 50.2 mW; modulation amplitude, 10 G; modulation frequency, 100 kHz; temperature, 77 K.

Facile chemical reduction of the 2-protonated−21-alkylated nickel(II) complexes such as **7**-HCl can be anticipated on the basis of the electrochemical data (Table 2). In fact, shaking a deaerated toluene/ethanol (10:1 v/v) solution of **7** with aqueous hydrazine dihydrochloride results in acidification of the complex causing appropriate changes of its optical spectrum[19] while appearance of an EPR signal indicates partial reduction of **7**-HCl (Figure 11). The metal-centered reduction and thus formation of d^9 nickel(I) ion can be inferred on the basis of the values of the Zeeman tensor components ($g_1 = 2.281$, $g_2 = 2.220$, $g_3 = 2.188$, toluene, 77 K) that differ considerably from those expected for a free radical.[25e,35,36] Similar result can be obtained upon reduction of **4**-HCl with $N_2H_6Cl_2$ ($g_1 = 2.294$ $g_2 = 2.220$, $g_3 = 2.181$, toluene, 77 K). In the case of a structurally related system, nickel(II) complex of 2,21-dimethylated inverted porphyrin **8**, reduction has been accomplished by a homolytic cleavage of the nickel−carbon bond with an apical alkyl or aryl ligand leading to a variety of EPR-active products.[22] The change in stability of the lower oxidation state in the case of **4**-HCl or **7**-HCl is related to the monoanionic character of the ligand upon protonation. Similar stabilization has been observed for nickel complexes of the other monoanionic core-modified porphyrins having oxygen, sulfur, or selenium replacing one nitrogen atom in the macrocyclic crevice.[25e,35−37]

Scheme 5 summarizes the redox behavior of the alkylated complexes under neutral and acidic conditions.

Conclusions

Modifications of the inverted porphyrin can be accomplished by introducing of various alkyl substituents on the internal carbon of the inverted pyrrole by means of readily available haloalkanes. Unlike in the case of regular porphyrins, where internal alkylation leads to monoanionic character of their coordination core, the alkylated inverted porphyrins can act as a bis-anionic ligands. In the case of nickel(II) complexes the unprotonated external nitrogen shows strong nucleophilic character which makes it capable for coordination of other metal ions. The flexibility of the system is reflected by proton-assisted change of spin state and accessibility of three different oxidation states of the metal ion.

A particularly attractive feature of the 21-alkylated systems is their chirality. The stereogenic center is localized within the coordination core, in the proximity of the ligation site of a potential substrate and the metal-localized redox center. It suggests application of these systems in stereoselective catalysis; however, further studies aimed on separation of enantiomerically pure complexes are required.

The potential variety in terms of the 21-C substituents is very large and allows for extremely facile design for specific purposes. Unlike in the case of chiral *N*-alkylated corroles, synthesis of which leads to a mixture of regioisomers (21-N and 22-N),[38,39] only one internally alkylated product is formed for the inverted porphyrin.

The mild dealkylation of some nickel complexes deserves particular attention, and the study proceeds to elucidate factors determining the C−C bond activation in these systems.

Scheme 5. Redox Properties of the Metal Center in Alkylated Inverted Porphyrin Nickel Complexes

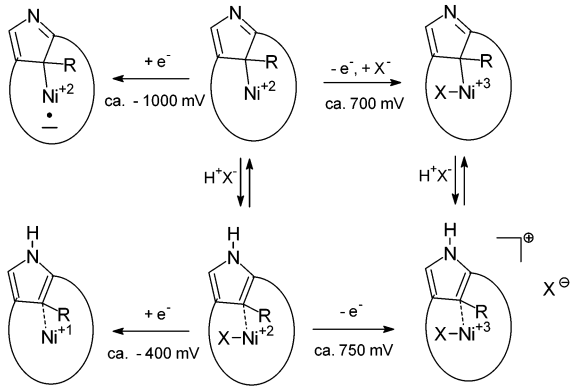

Experimental Section

Instrumentation. Absorption spectra were recorded on a diode-array Hewlett-Packard 8453 spectrometer. Mass spectra were recorded on an AD-604 spectrometer using the electrospray and electron impact techniques.

NMR spectra were recorded on a Bruker Avance 500 spectrometer. The 1D and 2D experiments (COSY, NOESY, HMQC, and HMBC) for diamagnetic substances were performed by means of standard experimental procedures of Burker library. For paramagnetic complexes usually 1000−10 000 scans were accumulated over a 10 kHz bandwidth with 32K data points and with a delay time of 100 ms. The signal-to-noise ratio was improved by apodization of the free induction decay, which typically induced 15-Hz broadening. The peaks were referenced against solvent resonances.

(35) Chmielewski, P.; Grzeszczuk, M.; Latos-Grażyński, L.; Lisowski, J. *Inorg. Chem.* **1989**, *28*, 3546.
(36) Chmielewski, P. J.; Latos-Grażyński, L.; Pacholska, E. *Inorg. Chem.* **1994**, *33*, 1992.
(37) Pacholska, E.; Chmielewski, P. J.; Latos-Grażyński, L. *Inorg. Chim. Acta* **1998**, *273*, 184.
(38) Jackson, A. H. In *The Porphyrins*; Dolphin, D., Ed.; Academic Press: New York, 1979; Vol. I, Chapter 8.
(39) Gross, Z.; Galili, N. *Angew. Chem., Int. Ed.* **1999**, *38*, 2366.

Cyclovoltammetric measurements were performed in dichloromethane on a EA9C MTM apparatus with glassy carbon disk as a working electrode, Ag/AgCl reference electrode, and platinum wire as an auxiliary electrode. Tetrabutylammonium perchlorate (0.1 M) was used as a supporting electrolyte.

EPR spectra were obtained with a Bruker ESP 300E spectrometer. The magnetic field was calibrated with a proton magnetometer and EPR standards. The EPR spectra were simulated by assuming orthorhombic symmetry. The details of the EPR simulations have been given elsewhere.[35,36]

Preparation of Precursors. 5,10,15,20-Tetraphenyl-2-aza-21-carbaporphyrin and (5,10,15,20-tetraphenyl-2-aza-21-carbaporphyrinato)nickel(II) (**1**) were synthesized according to known procedures.[5a,e]

Synthesis and characterization of complexes **10**−**16** were described previously.[23,24]

Synthesis of (5,10,15,20-Tetraphenyl-21-methyl-2-aza-21-carbaporphyrinato)nickel(II) (2). A mixture of **1** (30 mg, 0.045 mmol) and methyl iodide (45 mg, 0.32 mmol) in dichloromethane/ethanol solution (50 mL, 80/20, v/v) containing a suspension of K_2CO_3 was refluxed for 3 h under a blanket of nitrogen. The solvent was evaporated under reduced pressure. The solid was dissolved in dichloromethane and chromatographed on a silica gel column. The second brown-reddish band that contained **2** was eluted with dichloromethane and crystallized from a CH_2Cl_2/hexane mixture. Yield: 22 mg (71%). The mass spectroscopic, UV/vis, and NMR results are identical with the literature data.[19]

Synthesis of (5,10,15,20-Tetraphenyl-21-ethyl-2-aza-21-carbaporphyrinato)nickel(II) (3). A mixture of **1** (30 mg, 0.045 mmol) and ethyl iodide (45 mg, 0.29 mmol) in dichloromethane solution (50 mL) containing 2 mg of dibenzo-[18]-crown-6 and a suspension of K_2CO_3 (10 mg) was refluxed for 3 h under a blanket of nitrogen. The solvent was evaporated under reduced pressure. The solid was dissolved in dichloromethane and chromatographed on a silica gel column. The second brown-reddish band that contained **3** was eluted with dichloromethane and crystallized from a CH_2Cl_2/hexane mixture. Yield: 18 mg (57%). ^{1}H NMR (500 MHz, 298 K, $CDCl_3$; δ): 9.83 (1H, s, 3-H); 8.64 (1H, d, J_{AB} = 4.9 Hz); 8.62 (1H, d, J_{AB} = 4.9 Hz); 8.47 (2H, d, J_{AB} = 4.9 Hz); 8.43 (1H, d, J_{AB} = 5.7 Hz); 8.39 (1H, d, J_{AB} = 5.7 Hz); 8.22 (2H, b); 8.07 (2H, b); 8.02 (1H, b); 7.98 (1H, b) 7.8−7.6 (12H, overlapping multiplets); −0.93 (3H, t, J = 7.0 Hz, 2′-CH_3); −2.23 (2H, m, 1′-CH_2). ^{13}C NMR (125 MHz, 298 K, $CDCl_3$, partial data; δ): 179.4 (1-C); 154.5 (4-C); 156.5; 155.9; 152.8; 152.2; 140.6; 136.3; 133.8; 133.2; 128.0; 127.5; 127.3; 132.4; 38.6 (21-C); 24.8 (1′-C); 13.2 (2′-C). UV/vis (CH_2Cl_2) [λ_{max}, nm (log ϵ)]: 361 (4.29); 431 (4.60); 459 (sh); 550 (sh), 610 (sh), 759 (2.81) nm. HRMS (EI): m/z = 699.2537 (699.2059 for $C_{46}H_{32}N_4Ni$ + H^+).

Synthesis of (5,10,15,20-Tetraphenyl-21-(2′-hydroxyethyl)-2-aza-21-carbaporphyrinato)nickel(II) (4). A mixture of **1** (30 mg, 0.045 mmol) and 2-iodoethanol (100 mg, 0.6 mmol) in dichloromethane solution (30 mL) was allowed to stand in a darkness for 40 days. After that period solvent was evaporated under reduced pressure. The solid was dissolved in dichloromethane and chromatographed on a silica gel column. The second brown-reddish band that contained **4** was eluted with dichloromethane and crystallized from a CH_2Cl_2/hexane mixture. Yield: 13 mg (40%). ^{1}H NMR (500 MHz, 298 K, $CDCl_3$; δ): 9.73 (1H, s, 3-H); 8.63 (1H, d, J_{AB} = 5.0 Hz); 8.61 (1H, d, J_{AB} = 5.0 Hz,); 8.47 (2H, overlapping doublets, J = 5.0 Hz); 8.44(1H, d, J_{AB} = 5.0 Hz); 8.40 (1H, d, J_{AB} = 5.0 Hz); 8.22 (2H, b); 8.06 (2H, b); 8.02 (1H, b); 7.97 (1H, b); 7.8−7.6 (12H, overlapping multiplets); 1.56 (2H, m, J = 6.0 Hz, 2′-CH_2); −0,14 (1H, t, J = 6.0 Hz, OH); −2.42 (1H, m, 1′-CH_2); −2.56 (1H, m, 1′-CH_2). ^{13}C NMR (125 MHz, 298 K, $CDCl_3$, partial data; δ): 178.1 (1-C); 155.8 (3-C); 153.1 (4-C); 152.7 152.4; 140.1; 132.5; 133.5; 134.1; 132.2; 132.7; 128.0; 127.6; 126.6; 130.8; 61.7 (2′-C); 34.7 (21-C); 32.8 (1′-CH_2). UV/vis (CH_2Cl_2) [λ_{max}, nm (log ϵ)]: 354 (4.29); 432 (4.59); 462 (sh); 610 (sh), 751 (2.30). HRMS (EI): m/z = 714.1907 (714.1924 for $C_{46}H_{31}N_4ONi$ + H^+).

Synthesis of (5,10,15,20-Tetraphenyl-21-(*sec*-butyl)-2-aza-21-carbaporphyrinato)nickel(II) (5). This product was obtained in a way similar to that for **2** using 100 mg of 2-iodobutane instead of CH_3I and carrying out the reaction for 12 h. Yield: 19 mg (60%). ^{1}H NMR (500 MHz, 298 K, $CDCl_3$; δ): 9.76 (2H, s, 3-H, common signal for both diastereoisomers A + B); 8.64 (1H, d, J_{AB} = 5.1 Hz); 8.60 (1H, d, J_{AB} = 4.6 Hz); 8.58 (1H, d, J_{AB} = 4.6 Hz); 8.55 (1H, d, J_{AB} = 5.0 Hz); 8.48 (1H, d, J_{AB} = 5.0 Hz); 8.46 (1H, d, J_{AB} = 5.0 Hz); 8.45 (1H, d, J_{AB} = 5.0 Hz); 8.44 (1H, d, J_{AB} = 5.0 Hz); 8.43 (1H, d, J_{AB} = 5.0 Hz); 8.43 (1H, d, J_{AB} = 5.0 Hz); 8.42 (1H, d, J_{AB} = 5.0 Hz); 8.39 (1H, d, J_{AB} = 5.0 Hz); 8.38 (1H, d, J_{AB} = 5.0 Hz); 8.19 (8H, b); 8.03 (2H, d, J = 6.5 Hz); 7.84−7.56 (24H, overlapping multiplets); −0.37 (3H, 4′-CH_3 B); −0.41 (1H, m, 3′-CH (B)); −0.63 (3H, t, J = 7.3 Hz, 4′-CH_3 (A)); −0.74 (1H, m, 3′-CH (A)); −0.99 (1H, m 3′-CH (B)); −1.23 (3H, d, J = 6.4 Hz, 1′-CH_3 (A)); −1.62 (1H, m, 3′-CH (A)); −1.7 (3H, d, J = 6.9 Hz, 1′-CH_3 (B)); −3.55 (2H, m, 2′-CH, (A + B)) (assignments A and B introduced to distinguish signals of diastereoisomers). ^{13}C NMR (125 MHz, 298 K, $CDCl_3$, partial data; δ): 181.5 (1-C); 156.5 (3-C); 155.7(4-C); 152.4; 149.7; 148.5; 147.6; 146.6; 140.5; 135.7: 135.3; 134.5; 132.0; 133.6; 131.4; 128.1; 127.8; 127.2; 126.9; 44.7 (2′-C); 41.0 (21-C); 27.9 (3′-C (B)); 27.2 (3′-C (A)); 16.1 (1′-C); 12.5 (4′-C). UV/vis (CH_2Cl_2) [λ_{max}, nm (log ϵ)]: 358 (4.30); 435 (4.56); 469 (sh); 606 (sh), 734 (2.40). HRMS (EI): m/z = 727.2127 (727.2371 for $C_{48}H_{36}N_4Ni$ + H^+).

Synthesis of (5,10,15,20-Tetraphenyl-21-(*S*-2′-methylbutyl)-2-aza-21-carbaporphyrinato)nickel(II) (6). This product was obtained in way similar to that for **2** using 50 mg of *S*-(+)-2-(methyliodo)butane instead of CH_3I. Yield: 22 mg (66%). ^{1}H NMR (500 MHz, 298 K, $CDCl_3$; δ): 9.51 (1H, s, 3-H); 9.50 (1H, s, 3-H); 8.61 (2H, d, J_{AB} = 4.8 Hz); 8.58 (2H, d, J_{AB} = 5.0 Hz), 8.45 (2H, d, J_{AB} = 5.2 Hz.); 8.44 (1H, d, J_{AB} = 5.0 Hz.); 8.43 (1H, d, J_{AB} = 4.8 Hz.); 8.42 (2H, d, J_{AB} = 4.8 Hz.); 8.38 (2H, d, J_{AB} = 4.8 Hz.); 8.23 (4H, b); 8.10 (2H, b); 8.07 (2H, b); 8.01 (2H, b); 7.95 (2H, b); 7.85−7.60 (26H, overlapping multiplets); 0.03 (3H, t, J = 7.3 Hz, 4′-H (B)); −0.11 (1H, m, 3′ (B)); −0.12 (3H, t, J = 7.3 Hz, 4′ (A)); −0.23 (H, d, J = 6.7 Hz, 1″ (A)); −0.29 (1H, m, 3′ (A)); −0.37 (3H, d; J = 6.7 Hz, 1″-H (B)); −0.74 (2H, m, 2′-CH (A + B)); −1.81 (1H, dd, ^3J = 4.3 Hz, ^2J = 14.2 Hz, 1′ (A)); −2.26 (1H, dd, ^3J = 5.5 Hz, ^2J = 14.1 Hz 1′ (B)); −2.44 (1H, dd, ^2J = 14.1 Hz, ^3J = 6.4 Hz, 1′ (B)); −2,9 (1H, dd, ^2J = 14.2, ^3J = 7.8 Hz, 1′ (A)) (assignments A and B introduced to distinguish signals of diastereomers). ^{13}C NMR (125 MHz, 298 K, $CDCl_3$, partial data; δ): 178.3 (1-C); 155.7 (3-C); 155.4; 154.4 (4-C); 152.7; 149.8; 147.7; 140.1; 139.7; 136.8; 135.9; 133.7; 133.3; 132.7 132.3; 132.0 127.8; 127.2; 40.9 (21-C); 35.5 (1′-C (A + B)); 36.5 (2′-C (A + B)); 29.5 (3′-C (A)); 28.4 (3′-C (B)); 19.5 (1″-C (B)); 18.8 (1″-C (A)); 10.8 (4′-C (A + B)). UV/vis (CH_2Cl_2) [λ_{max}, nm (log ϵ)]: 359 (4.30); 434 (4.58); 465 (sh); 608 (sh), 740 (2.30). HRMS (ESI): m/z = 741.2528 (741.2523 for $C_{49}H_{38}N_4Ni$ + H^+).

Synthesis of (5,10,15,20-Tetraphenyl-21-benzyl-2-aza-21-carbaporphyrinato)nickel(II) (7). This product was obtained in way similar to that for **3** using 100 mg of benzyl chloride instead of C_2H_5I and refluxing the reaction mixture for 12 h. Yield: 27 mg (80%). ^{1}H NMR (500 MHz, 298 K, $CDCl_3$; δ): 9.56 (1H, s, 3-H); 8.72 (2H, d, J_{AB} = 4.9 Hz); 8.55 (1H, d, J_{AB} = 4.6 Hz); 8.54 (1H,

d, $J_{AB} = 4.9$ Hz); 8.47 (1H, d, $J_{AB} = 4.6$); 8.43 (1H, d, $J_{AB} = 4.9$); 8.13 (3H, b); 8.04 (1H, b); 8.00 (2H, b); 7.8−7.6 (12H, overlapping multiplets); 7.00 (1H, m, *para* (benzyl)); 6.92 (2H, m, *meta* (benzyl)); 5.55 (2H, m, *ortho* (benzyl)); −1.28 (1H, d, $^2J = 13.8$ Hz, 1′-H); −1.57 (1H, d, $^2J = 13.8$ Hz, 1′-H). ^{13}C NMR (125 MHz, 223 K, $CDCl_3$; δ): 177.6 (1-C); 157.2 (3-C); 155.9; 153.1 (4-C); 152.6; 150.2; 149.5; 147.6; 146.8; 140.7; 140.5; 139.6 (*ipso*-benzyl); 139.4; 138.0; 137.5; 137.1; 135.6; 135.5; 134.7; 134.4; 134.3; 133.9; 133.7; 133.6; 133.0; 132.6; 132.5; 132.2; 131.8; 128.8; 128.1; 128.0; 127.8 (*o*-benzyl)); 127.6 (*m*-benzyl); 127.4 (*p*-benzyl); 126.9; 126.0; 125.1; 123.5; 38.4 (21-C); 35.4 (1′-C). UV/vis (CH_2Cl_2) [λ_{max}, nm (log ϵ)]: 358 (4.40); 433 (4.60); 461 (sh); 605 (sh); 762 (2.63). HRMS (ESI): $m/z = 761.2183$ (761.2215 for $C_{51}H_{34}N_4Ni + H^+$).

Synthesis of 5,10,15,20-Tetraphenyl-21-benzyl-2-aza-21-carbaporphyrin (17). A solution of **7** (10 mg, 0.013 mmol) in dichloromethane (10 mL) was shaken for 3 min with 1 mL of concentrated hydrochloric acid and then neutralized with saturated aqueous potassium carbonate. The organic layer was separated, dried with anhydrous potassium carbonate, and chromatographed on the basic alumina column with dichloromethane as an eluent. Crystallization from a benzene/hexane mixture gave 7 mg of **17** (yield 75%). ^{1}H NMR (500 MHz, 298 K, $CDCl_3$; δ): 8.76 (1H, d, $J_{AB} = 4.9$ Hz); 8.68 (1H, d, $J_{AB} = 4.9$ Hz); 8.49 (3H, overlapping doublets); 8.42 (1H, d, $J_{AB} = 4.9$ Hz); 8.28 (2H, m); 8.24 (1H, m); 8.18 (2H, b); 8.15 (3H, m); 8.10 (1H, m); 7.81 (2H, m); 7.77 (2H, m); 7.73 (9H, overlapping multiplets); 7.14 (1H, s, 3-H); 6.42 (1H, m, *para* (benzyl); 6.27 (2H, m, *meta* (benzyl)); 4.33 (2H, m, *ortho* (benzyl)); −2.55 (2H, b, 22,24-NH), −3.53 (1H, d, $^2J = 16.5$ Hz, 1′-H); −3.79 (1H, d, $^2J = 16.5$ Hz, 1′-H). ^{1}H NMR (500 MHz, 233 K, $CDCl_3$; δ): 8.80 (1H, d, $J_{AB} = 4.9$ Hz); 8.72 (1H, d, $J_{AB} = 4.3$ Hz); 8.53 (3H, overlapping doublets); 8.48 (1H, d, $J_{AB} = 4.3$ Hz); 8.28 (1H, m); 8.19 (4H, overlapping multiplets); 8.13 (1H, m); 7.91 (1H, b); 7.83 (1H, m); 7.81 (1H, m); 7.76 (11H, overlapping multiplets); 7.12 (1H, s, 3-H); 6.40 (1H, m, *para* (benzyl)); 6.25(2H, m, *meta* (benzyl)); 4.25(2H, m, *ortho* (benzyl)); −2.79 (1H, b, NH); −2.88 (1H, b, NH); −3.63 (1H, d, $^2J = 16.5$ Hz, 1′-H); −3.94 (1H, d, $^2J = 16.5$ Hz, 1′-H). ^{13}C NMR (125 MHz, 233 K, $CDCl_3$; δ): 157.6; 156.8 (1-C); 150.7; 141.4; 141.3 (3-C); 140.2; 139.6; 139.4; 138.8; 137.9 (4-C); 137.1 (*ipso* (benzyl)); 136.4; 136.3; 135.2; 135.1; 134.8; 134.7; 128.7; 128.5; 128.4; 127.9; 127.81; 127.79; 127.7; 127.63; 127.58; 127.4; 127.3; 127.0; 126.98; 126.9; 126.8; 126.3; 126.2 (*meta* (benzyl)); 125.65 (*ortho* (benzyl); 125.6; 124.5 (*para* (benzyl)); 118.3; 116.9; 106.6 (21-C); 27.9 (1′-C). UV/vis (CH_2Cl_2) [λ_{max}, nm (log ϵ)]: 449 (4.93); 515 (3.92); 551 (4.01); 594 (4.00); 691 (sh); 743 (3.80). HRMS (ESI): $m/z = 705.2996$ (705.3013 for $C_{51}H_{37}N_4 + H^+$).

Synthesis of 2-(21′-(5′,10′,15′,20′-Tetraphenyl-2′-aza-21′-carbaporphyrin)methyl)-5,10,15,20-tetraphenyl-2-aza-21-carbaporphyrin (18). This ligand was obtained similarly as **17**, but the dichloromethane solution of starting complex **10** was stirred with concentrated HCl for 2 h. Yield: 60%. ^{1}H NMR (500 MHz, 233 K, $CDCl_3$; δ): 8.70 (1H, d, $J_{AB} = 4.9$ Hz); 8.57 (1H, d, $J_{AB} = 4.6$ Hz); 8.54 (1H, d, $J_{AB} = 4.1$ Hz); 8.47 (1H, d, $J_{AB} = 4.1$ Hz); 8.44 (1H, d, $J_{AB} = 4.1$ Hz); 8.32 (1H, d, $J_{AB} = 4.1$ Hz); 8.29 (1H, m); 8.26 (1H, m); 8.13 (1H, d, $J_{AB} = 4.1$ Hz); 8.02 (2H, m); 7.93 (1H, d, $J_{AB} = 4.6$ Hz); 7.91−7.70 (overlapping multiplets); 7.68 (2H, two overlapping doublets scalar coupled with 23-NH); 7.56 (2H, m); 7.50 (1H, m); 7.47 (1H, d, $J_{AB} = 4.6$ Hz); 7.41 (2H, b); 7.12 (1H, d, $J_{AB} = 4.6$ Hz); 6.93 (1H, d, $J_{AB} = 4.1$ Hz); 6.71 (1H, s, 3′); 6.31 (1H, m); 6.03 (1H, m); 5.96 (1H, m); 5.77 (1H, m); 5.65 (1H, s, 3); 5.58 (1H, m); 3.16 (1H, s, 2-NH); 0.15 (1H, s, 21-CH); −2.42 (1H, d, $J_{AB} = 16.0$ Hz); −2.74 (1H, d, $J_{AB} = 16.0$ Hz); −3.28 (2H, b, 22′,24′). UV/vis (CH_2Cl_2) [λ_{max}, nm (log ϵ)]: 439 (4.63); 467 (sh); 557 (3.40); 608 (3.70); 682 (sh); 737 (3.80). MS (ESI): $m/z = 1241.3$ (1241.5 for $C_{89}H_{60}N_8 + H^+$).

Acknowledgment. This work was supported by the State Committee for Scientific Research of Poland (Grant Nos. 7 T09A 120 20 and 4 T09A 147 22).

IC034096K